DEVELOPMENT OF LIGHT WEIGHT ALUMINIUM METAL MATRIX COMPOSITE BY STIR CASTING PROCESS

A PROJECT REPORT

Submitted in partial fulfillment of the requirement for the award of the degree of

MASTER OF TECHNOLOGY

in

PRODUCTION ENGINEERING

by

RAHUL KHURANA

Roll No. 2K14/PIE/12

Under the guidance of

Dr. R.S. WALIA
Associate Professor
Department of Mechanical Engg.
DTU, New Delhi

Dr. M.S. NIRANJAN
Assistant Professor
Department of Mechanical Engg.
DTU, New Delhi

Department of Mechanical Engineering,

Delhi Technological University, New Delhi (110042)

(Formerly Delhi College of Engineering)

Department of Mechanical Engineering

Delhi Technological University

Delhi

CERTIFICATE

This is to certify that the thesis entitled **"Development of Light Weight Aluminium metal matrix composite by Stir Casting process."** submitted by **Rahul Khurana (2K14/PIE/12)**, during the session 2014-2016 for the award of M.Tech degree of Delhi Technological University, Delhi is absolutely based upon his work done under our supervision and guidance and that neither this thesis nor any part of it has been submitted for any degree/diploma or any other academic award.

The assistance and help received during the course of investigation have been fully acknowledged. He is a good student and we wish him good luck in future.

Dr. R.S. Walia
Associate Professor
Department of Mechanical Engg.
DTU, Delhi

Dr. M.S. Niranjan
Assistant Professor
Department of Mechanical Engg.
DTU, Delhi

ACKNOWLEDGEMENT

I would like express my deep sense of respect and gratitude to my mentors, Dr. R.S. Walia and Dr. M.S. Niranjan (Dept. of Mechanical Engg., DTU, Delhi) for their invaluable and fruitful constructive suggestions and guidance that have enabled me to overcome all the problems and difficulties while carrying out my research work. I feel fortunate for the support , involvement and well wishes of my mentors and this is virtually impossible to express them in words.

I express my sincere gratitude and indebtedness to Dr. Qasim Murtaza for his valuable support and guidance , his timely suggestions were always beneficial. I would also like to thank N. Yuvraj sir for his help and advice on various aspects of research work.

In the end I would thank all the DTU staff for letting me use the labs for testing part and helping me out on various occasions where I would have been stuck without their help.

I deeply acknowledge my indebtedness to my parents, for their love who always supported me and helped me. And to my friends for their support, good wishes and continuous engagement.

And I would specially thank Dr. R.S. Walia for always helping me out and being there in difficult situations, for showing me path to good work and being a good person

Rahul Khurana

2K14/PIE/12

M.Tech Production Engineering

Delhi Technologoical University

CONTENTS

LIST OF TABLES

LIST OF FIGURES

ABSTRACT

In recent years, the developments of metal matrix composite (MMCs) have been receiving worldwide attention on account of their superior strength and stiffness. They also have high wear resistance and creep resistance in comparison to their corresponding wrought alloys. The existing process to fabricate, characterize and machine this special material needs improvement. Although, some attempts have been made to machine these materials but no suggestion has been made so far about the optimum value of cutting parameters for a particular type of MMC. Optimum value of cutting parameters will be different for different MMCs. Some categories of these MMC find applications in aircraft and space industries, where precise machining is most important. Hence, there is a need to develop a process for precise, energy efficient and cost effective machining. So that Aluminium composites for light weight applications can be fabricated cost effectively.

So this study is aimed at low cost fabrication of Aluminium metal matrix composite with Boron carbide (B_4C) as dispersed phase and AA7075 as matrix phase which can be used in various light weight applications by using 'Stir Casting' method. The developed composite shows improved tensile and yield strength along with increase in vicker's hardness. The microstructure studies have also been carried out which uniform distribution of reinforcement particles, phases made after development of composite and also the reduction in grain size. The wear test was also done which revealed favorable results. Further optimization of machining results has been done for studying the effect of speed, feed and depth of cut. The results have been compared with the results of as-casted AA7075.

CHAPTER-1

INTRODUCTION

A composite material is a material system which is composed of a suitably arranged mixture or grouping of two or more nano, micro, or macro constituents with an interface separating them that differ in form and chemical composition and are essentially insoluble in each other. The discrete constituent is called as the reinforcement and the continuous phase is called as the matrix. According to the chemical nature of the matrix phase, composites are classified as metal matrix (MMC), polymer matrix (PMC) and ceramic matrix composites (CMC). MMC's recently are capturing interests of the researchers because of the ability to change their physical properties like density, thermal diffusivity, thermal expansion and mechanical properties like tensile and compressive behavior, creep, tribological behavior etc. by changing the reinforcement phase.

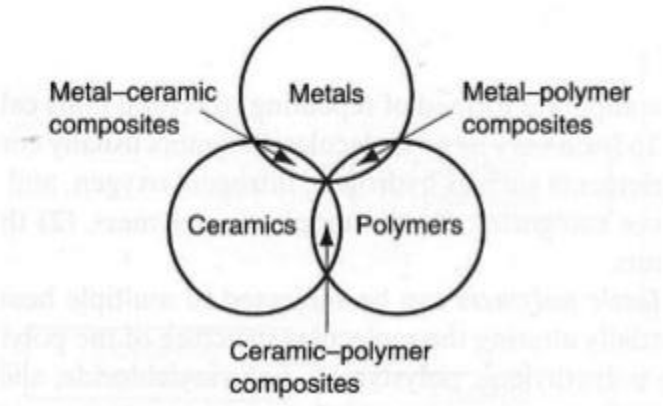

Figure 1.1: Venn diagram showing basic material types plus composites.

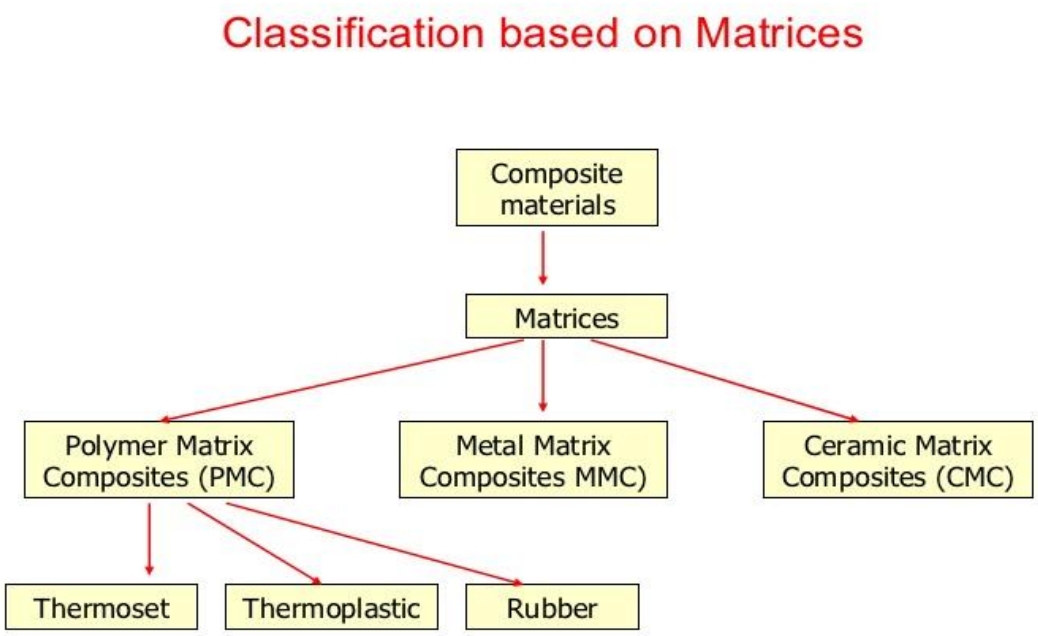

Figure 1.2: Classification of composites based on matrices.

In the recent past the need for low cost, high strength and good quality materials has augmented worldwide. Combination of high specific strength along with good corrosion resistance, metal matrix composites (MMCs) are materials that are eye-catching for a large range of general as well as engineering applications. Among MMC's , aluminium metal matrix composites (AMMC) due to their low cost compared to other materials, high wear resistance as well as high ratio of strength to weight are extensively fabricated for use in structural applications as well as in automobile and aerospace industry. However their relatively high cost of fabrication has restricted their widespread use. And this problem is due to lack of inexpensive fabrication technique for producing high quality MMC's on mass scale.

Therefore a simple and cost effective method for fabrication of aluminium composites is very much essential for their vast field of application. Depending on the choice of matrix

used and reinforcement chosen, fabrication techniques vary considerably. These methods can mainly be divided into 3 main categories: liquid state, solid state and semi-solid state processes. Generally solid state processes are used to get better mechanical properties in case of MMCs, especially discontinuous MMCs. It is because intermetallic phase formation and segregation effect are comparatively less in these processes, when compared to liquid state processes. **[1]**

Stir casting method is widely accepted and now a day's used commercially for manufacturing of AMMC's. . So this study is aimed at low cost fabrication of Aluminium composite which can be used in various light weight applications by using 'Stir Casting' method.

1.1 Stir Casting: This method of fabricating MMCs basically involves producing selected matrix material's melt which is then followed by introduction of dispersed phase i.e. reinforcement material. The dispersion of reinforcement material is then carried out by mechanical stirring of the mixture.

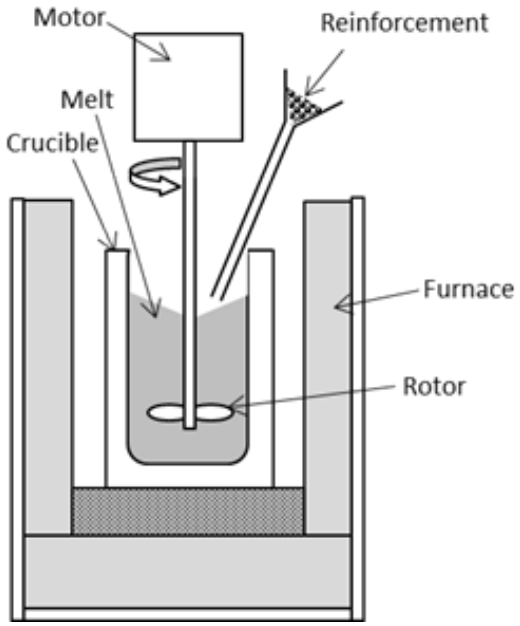

Figure 1.3: Basic principle of Stir Casting Method.

The advantages of Stir casting method lies in the flexibility, simplicity and applicability it offers while producing large quantities of composite. Various types of ceramic reinforcements like silicon carbide, boron carbide, particulate alumina, graphite, fly ash etc can be used in fabrication of AMMC's. Also organic reinforcements like rice husk ash, coconut coir's ash, fly ash etc can also be used.

Besides these advantages there are various problems associated with production of Aluminium MMCs by this method.

1.1.1 Problems associated with Stir Casting

There are various problems associated with stir casting method and some of the factors need significant attention. These are:

1. The level difficulty involved in achieving uniform distribution of dispersed phase i.e. reinforcement into matrix alloy.
2. Wettability of reinforcement material which is in solid state by matrix alloy's melt.
3. Porosity defect in casted MMC.
4. Chemical reaction may take place between the matrix alloy and reinforcement material.

For achieving the optimum properties the distribution of the reinforcement should be uniform into matrix alloy. The wettability should be optimized between the materials. The porosity should be minimum and chemical reaction should be avoided between the materials by employing various techniques.

Due to density difference between the two materials, the reinforcement particles tend to settle down during holding of melt or while casting. Dispersion of reinforcement particles is also affected by pouring temperature and pouring rate. A successful casting should have proper distribution of particles throughout metal matrix. For this to take place both the materials should be preheated at a certain temperature so as to remove all the moisture as well as air which is trapped between the particles. The stirrer speed should not be too low or too high and stirring should take place for few minutes continuously. **[2]**

Wettability is the liquid's ability to spread on the surface of solid. For successful incorporation of reinforcement particles into casting needs the melt to wet the solid phase of ceramic. The wetting can be improved by reducing surface tension of molten matrix alloy and by increase of the surface energy of the solid. There are various method to

achieve the same, one is by heat treating of particles before dispersing them into melt as it causes desorption of gases adsorbed from the surface of particle. As the size of particles decreases, achieving wettability becomes more difficult because of increase in surface energy which is needed for the surface of metal to be deformed to smaller radius when the penetration of particles begins through it. Also the fine powder tends to agglomerate together as the particle size goes on increasing. **[2]**

The problem of porosity cannot be avoided fully but can be controlled. The main causes of porosity are entrapment of gases during mixing, evolution of hydrogen and solidification shrinkage. There are various methods to minimize porosity but for aluminium degassing of liquid melt is best.

In this work, MMC having 7075Aluminium alloy (AA7075) as matrix and Boron carbide (B_4C) as reinforcement, has been identified, since it has potential applications in aircraft and space industries because of lower weight to strength ratio, high wear resistance. And the method chosen for fabrication of composite is 'stir casting method'. Since it is cost effective and by controlling the parameters like melting temperature, stirring speed, stirring time and position of stirrer defect free casting is produced. Composites with AA7075 with 8% B4C by wt. were produced. And the Characterization of samples was done by following tests; scanning electron microscope (SEM), Energy dispersive X-ray analyses (EDAX), microstructure analysis by high resolution microscope, X- Ray Diffraction Analysis (XRD). Mechanical properties have been investigated by tensile test, and hardness test. Lathe machine has been used for machining of composite. Carbide insert tool has been used for machining the composite. Also the spectro analysis test was done base AA7075 for surety of original alloy.

CHAPTER-2

LITERATURE REVIEW

This chapter deals with literature review related to stir casting process, material characterizations, mechanical properties, machining parameters etc. Certain gaps have also been identified in the literature review.

2.1 STIR CASTING PROCESS AND SET UP STUDIES

Due to difference in properties like density, boiling point and melting point of ceramic materials as compared to metals, non-uniform particle distribution is one the biggest problems in fabrication of MMCs by stir casting method.

Hashim et al. **[2]** discussed about various methods of reinforcement introduction into the melted matrix, so as to properly disperse them. Among the various methods discussed, vortex method is better approach for creating as well as maintaining a proper distribution of particles in the matrix alloy. In this method the melt is stirred vigorously so as to form a vortex at the melt's surface and then the reinforcement is to be added on the vortex's side. The stirring mechanism has mainly two benefits i.e. distributing of particles into the melt and to continuously the keep the reinforcement particles in suspension state into the liquid melt. Due to development of vortex the pressure difference is created between the outer and inner surface of liquid melt as a result of which reinforcement particles are sucked into the liquid. However drawback of this is that air bubbles and other impurities which are present on the surface of the liquid are also sucked into the melt due to the same mechanism. This results in high level of porosity and inclusion into the composite casted. And these gases are very difficult to remove as the viscosity of mixture increases. Therefore stirrer should be designed so as to avoid agitation and vortex formation on the surface of the melt. The stirring should be continuous before pouring and its speed should be optimum.

Naher et al. **[3]** simulated the Stir casting process. Some parameters were optimized for uniform particle distribution. The simulation involved visualisation experiments in which

liquid and semi solid aluminium were replaced by other fluids with similar characteristics and similar to SiC reinforcement particulate were used simulation fluid mixtures. Optimum conditions for photographing flow patterns were established. At 50 rpm no dispersion of the particles was observed irrespective of blade angle or fluid. And at 100 rpm and with 0 and 30 degree blade angles no uniform dispersion resulted, but with 45 and 60 degree blade angles there was full particulate dispersion. It was also observed that for all stirring speeds that dispersion rates increased with increasing blade angle. Below 150 rpm no dispersion was observed for the higher viscosity glycerol/water mixtures. It was found that for most cases the 60 degree angle produced the lowest dispersion times. The turbine stirrer also gave the lowest dispersion times. With increase in the height of the stirrer in the melt, the dispersion times increased. It was also observed that 4 blade stirrer to produced shorter stirrer times than the 3 blade stirrer. Air entrapment was also observed in all fluids at speeds above 250 rpm, though it was surprisingly more evident in the higher viscosity fluids. Higher blade angles and lower viscosity result in reduced particulate dispersion time.

Sekar et al. **[4]** designed the stir casting setup for light weight metals like aluminum, copper and magnesium. Proper calculations were done for stirrer speed, die design, nano particle pre heater design and heating vessel design. Pre heater was attached in top of furnace and set up is designed to tackle the issue of wettability of particles by introduction of tapered pathway heater pipe directly into the crucible.

Thomas.A et al. **[5]** designed, fabricated and tested different stirring and feeding mechanism by producing Aluminium composite with SiC particles. Identification of best mechanism was done by testing each of them individually. Results obtained from tensile test and hardness for different samples show that uniform controlled spraying of SiC particles was improved by the modifications done on feeding mechanism. And better flow patterns which ensured uniform distribution of SiC particles in the composite obtained by the modifications done on dimension and geometry of stirrer.

Juang et al. **[6]** performed experiments to study the effect of preheating temperature and the rate of adding reinforcement particles on the distribution in aluminium composite. The reinforcement chosen was fly ash. During the experiments the fly ash was pre heated

different set of temperatures i.e. 400°C, 500°C, 600°C, 660°C, 700°C and 800°C. The flow rates chosen for introduction of particles were 0.10 g/s, 0.15 g/s, and 0.2 g/s. Experimental results show that preheating temperatures were helpful in the dispersion of fly ash particles into the melt as well as it also increased the rate of chemical reaction between the materials i.e. aluminum and fly ash. And by increasing the rate of addition led to formation of cluster and proper dispersion of fly ash particles was constrained. At lower rates the dispersion was better and it allowed more time for occurrence of chemical reaction. Also higher preheating temperatures and lower rates of addition significantly reduced the porosity which may be due to prevention of clustering of particles. At preheating temperature of 800°C and addition rate of 0.10 g/s the lowest level of porosity content i.e. 1.04% was noted.

2.2 MATERIAL CHARACTERIZATIONS

Beffort et al. **[7]** studied the effect of alloying and age hardening for $AlCu_3$ and $AlZn_6Mg_1$ as well as the specific role of Mg additions to Al/SiC MMCs on interface microstructure formation, mechanical properties and fracture mode. While using squeeze casting, assisted pressurization for the infiltration of SiC particle preformed with high purity Al, the formation of Al_4C_3 is widely prevented. This is due to the peculiarities of the squeeze casting process which does not provide favorable thermodynamic and kinetic conditions for the associated reaction to proceed. However, under identical process conditions, additions of Mg lead to the formation of both Al_4C_3 and Mg_2Si. Si which is released from the direct reaction between Al and SiC reacts with Mg to form Mg_2Si. This reaction, in turn, decreases the Si activity and, thus favours the formation of Al_4C_3 in squeeze cast AlMg/SiCp composites. Any potential positive effect of enhanced interfacial bonding strength due to the Mg addition on mechanical properties is counterbalanced by the embrittling effect of the interfacial reaction products.

Barman et al. **[8]** studied the evolution of microstructure during solidification of A356 alloy whose stirring was performed in a high temperature concentric viscometer. The variation of the slurry viscosity with fraction of solid during solidification was also studied.

During solidification the the stirring results in semisolid slurry in the annular space between the cylinders which is removed time to time during processing with the help of vacuum removal quartz tube and then it is quenched in water for further analysis. The constant cooling rate of 1 °C/min and shear rate of 150 s^{-1} was used to obtain the semi solid slurry. When liquid alloy which is above liquidus temperature before quenching is solidified dendritically without stirring in the quartz tube then only dendritic structure is obtained. When temperature in viscometer goes below liquidus temperature fragmented dendrites are formed at surface of cylinder which are transported into the melt by the stirring action. When the temperature of slurry is near liquidus temperature the fragmented dendrites are fewer and more spatially distributed this result in low viscosity of slurry in the early stage of solidification. But as the temperature decreases further the fragmented dendrites present in the slurry start increasing in number and become coarsened, as a result the viscosity of the slurry increases as the temperature decreases. It is observed in that the viscosity increases at a very low rate at the beginning of the solidification, but rapidly increases when the fraction of solid is about 0.4–0.55.

Ezatpour et al. **[9]** prepared MMC with Al6061 alloy in which nano Al_2O_3 were introduced by powder injection of Al/Al_2O_3 and then extrusion process was used to get the desired shape. The composites were prepared with varying percentage of reinforcement i.e. 0.5, 1 and 1.5 wt. % of Al_2O_3. The images obtained from SEM and optical microscopy indicate reduction in grain size of aluminium matrix with addition of Al_2O_3 and also the grain size decreases with increase in volume fraction of nano particles. It is because grain growth is prevented due to higher incidence of grain boundary pinning. Also the porosity increased with increasing content of alumina. But SEM images also reveal improvement of microstructural densification, lowering of porosity, grain refining, and grain orientation in the hot-extruded direction i.e. porosity decreased by use of extrusion process. Extrusion resulted in low agglomeration of nano particles due to which more homogenous dispersion of particles was obtained throughout the matrix.

Hassan et al. **[10]** studied the effect of eggshell on properties and microstructure of Al–Cu–Mg/eggshell particulate composites. Eggshell particles were added in varying percentage of 2–12 wt.%. The particles were added both in carbonized and uncarbonized form and

comparison was made among both of them with help of different mechanical testing. The microstructure of particles (Uncarbonized and Carbonized) shows the variation in shape and size though they consist of they consist of porous irregular shaped particles. The EDS of particles confirmed the presence of Ca, Si, O, C, Mg, p with the presence of C in the carbonized eggshell particles. This test confirms the presence of calcium carbonate in the form of calcite (CaCO3), the carbonized ES have carbon in graphite form. The microstructure study shows the eutectic phase containing Cu_3Al_2, Al_6CuMg_4 in α-aluminium matrix. In the Al–Cu–Mg alloy, Cu and Mg are present both in solid solution as well as in precipitated form as Cu_3Al_2, and Al_6CuMg_4 phases both in the grain and along the grain boundaries. Uniform distribution of particles is also confirmed by microstructure study. The particles got distributed along the grain boundaries of alloy in the composite but the grain size of composite gets reduced as compared to matrix alloy. The energy dispersive spectrometer (EDS) analysis indicates towards possible chemical reaction between aluminium melt and ES particles which led to the release of Si, Na, O, C and Ca etc., in the composites. Also the presence of the carbonized eggshell particles resulted in a much smaller grain size in the composites compared to uncarbonized eggshell composites which is due to smaller particles and great fineness of carbonized eggshell than uncarbonized eggshell particles. Also the decrease in density with increasing percentage of particles was observed. The density of the composites decreased from 2.78 g/cm3 at 0 wt. % to 2.57 g/cm3 and 2.50 g/cm3 at 12 wt.% for uncarbonized and carbonized ES particles, whereas the density of uncarbonized and carbonized Eggshell particles was 2.47 and 1.98 g/cm3, respectively. This shows that light weight composites can be made by using ES particles.

Valibeygloo et al. **[11]** analyzed the effect of alumina nanoparticles on Al-4.5wt% Cu alloy with varying volume fraction of alumina particles (1.5vol%, 3vol%, and 5vol%) on composite fabricated by stir casting method. The alumina nanoparticles were ball milled with aluminium powders in a planetary ball mill for duration of 5 hours, and then packets of these powders were added during stirring. Results show that milling of powders increase wettability of particles with the melt by a considerable amount. Because of ball milling, Al_2O_3 particles are stuck between Aluminium particles, and actually, Al particles, take the role of carrier for alumina particles, improve the wettability. The SEM images confirm the

presence of gas holes due to due to the sticking of environmental gases and suction of air bubbles into the melt during casting. It also shows that particles act as the homogeneous nucleation sites and with the increase in volume fraction of reinforcement clustering of particles increases and efficiency of particles entering into the melt decreases. Grain growth and porosities were observed due to the trapping of gases into the melt. EDX spectra results indicate the presence of Al_2Cu and Al_2O_3 phases in the microstructure.

Suresh et al. **[12]** studied the effect of TiB_2 on aluminium alloy 6061. MMCs were prepared with different weight fractions of TiB_2 i.e. 0, 4, 8 and 12% by stir casting method. Morphological features were investigated with help of SEM analysis of TiB_2 particles. TiB_2 particles exhibit different shapes such as spherical, hexagonal and cubic. The images show clear interface presence which can be credited to formation of particles within the melt itself and thermodynamic stability of the TiB_2 particles. Thermodynamically unstable behavior of ceramic particle in molten aluminium, produces unwanted compounds at the interface of matrix and particle. The load bearing capability of aluminium metal matrix composite is increased with the presence of pure interface. Also the mechanical as well as tribological properties are enhanced. The SEM images of worn surfaces obtained by wear testing clearly indicate the abrasive wear as primary wear mechanism. Comparison of wear surfaces of alloy and composite show difference in patterns of grooves and scars which can be attributed to poor wettability, insufficient stirring and density variation between ceramic particle and matrix alloy. Also the images clearly show the absence of defects like porosity and shrinkage cavity which is good for improving elongation, strength and plastic modulus. SEM- EDS analysis was also performed which confirms the presence of boron, titanium and aluminium.

2.3 MECHANICAL PROPERTIES

2.3.1 Tensile strength, Fracture behavior and Hardness

The 7075 aluminum alloy is widely used in the aerospace applications for its light weight and high stiffness. To further improve the mechanical properties, particle or whisker-reinforced 7075 MMCs can be developed. The mechanical properties and deformation behavior of these MMCs are quite different from their base alloys. Ceramic particles in the

ductile matrix lead to the desirable properties. These properties include increased strength, higher elastic modulus, higher service temperature, improved wear resistance, decreased part weight, low thermal shock, high electrical and thermal conductivity

Campos et al. **[13]** fabricated nanostructured composites of aluminum alloy Al7075 and carbon coated silver nanoparticles with help of mechanical milling and indirect hot extrusion. High energy SPEX ball mill was used to get the milling products which were then compacted by uniaxial load and pressure-less sintered under argon atmosphere. Finally, the sintered product was hot extruded. Results show that the microhardness of the as-milled composites increases with increments in the milling time. It was observed that the nanostructured composites produced in this work, exhibit superior values than those observed in the Al7075 alloy in the T73 and T6 condition. On the other hand, with increments in the content of the Ag–CNP's, the microhardness increased and showed maximum values (~300 HVN) between 1.0 and 1.5 wt.%, and then decreased to lower values (~200 HVN). These increments were due to uniform distribution of nanoparticles into the matrix. Tensile test results show that milling time and nanoparticle's content did not have much effect on the yield strength of the unreinforced alloy. However, the values found in unreinforced samples in the as-milled condition present an increase of ~80% than the one reported for the same alloy in annealed condition. Fractography results of broken surfaces after tensile test of the hot-extruded samples show ductile fracture with dimples sizes of about 2–5 μm for the content of the three nanoparticles.The best mechanical properties were obtained at 1.0–1.5 wt. % of Ag–C NP's and a 10 h milling. The dispersion of silver nanoparticles and crystallization of phases were the main factors that caused the increase in the mechanical properties.

Saravanan et al. **[14]** used rice husk ash (RHA) with aluminium alloy (AlSi10Mg) to develop composite by stir casting method. Different volume fraction of ash i.e. 3, 6, 9 & 12 % by weight were used. RHA particles were preheated to a temperature of 600 °C for 3 hours and mixed at the temperature of 800 °C into the melt. Stirring was done speed of 500 to 700 rpm. Tensile strength of composites increased with an increase in the weight percentage of RHA as the RHA particles act as barriers to the dislocations in loading condition. However beyond 12% weight fraction of RHA, the tensile strength decreased

which may be due to the poor wettability of the particles with the melt. Compressive strength also increased with an increase in the weight percentage of RHA particles due to the hardening of the base alloy by rice husk ash particles. The hardness of the composite increased linearly with the increase in weight fraction of the RHA particles. But the ductility of the composite decreased with the increase in weight fraction of the RHA which is due to the increase in hardness or clustering of RHA particles.

Kumar et al. **[15]** fabricated composite by adding Al_2O_3 to Aluminium A359 by electromagnetic stir casting process. Here the melt was electromagnetically stirred by using a 3-phase induction motor after addition of the pre-heated Al_2O_3 particles (about 800 °C). The different volume fraction of alumina used was 2 wt. %, 4 wt. %, 6 wt. %, 8 wt. % with average particle size of 30 μm. The mixing was done at 750 °C with stirring speed of 300 rpm. Hardness test was conducted with load of 60 kgf and a steel ball of diameter 2.5mm as indenter and Rockwell hardness was obtained. The data show that hardness value increased with increase in particle content. The maximum hardness value obtained at 8 wt. % of Al_2O_3 which was about 58% higher than the matrix metal. The tensile strength of the composites was improved by addition of Al_2O_3 and it increased with increase in volume fraction of particles. The tensile strength of non-reinforced A359 alloy was about 103.7 N/mm^2 and it increased to a maximum of 148.7N/mm2 for A359/Al2O3/8 wt. % which is about 45% higher. However, percentage elongation reduced as the brittleness of the metal increased. The tensile strength increased due to refinement of the grain size of aluminum and hence increase in amount of grain boundary during the solidification process.

Akbari et al. **[16]** investigated the effect of reinforcement of TiB_2 nano and microparticles in A356 aluminum matrix on tensile and fracture behavior. Micro and nano titanium diboride powders with average sizes of 20 nm and 5 μm was used in different volume fractions. Casting temperature of 750, 800 and 900 °C was used to fabricate different composites. Volume fraction of 0.5, 1.5, 3, and 5 vol. % of nano and micro TiB_2 powders were used for fabrication of composite. Stirring was done at 450 rpm for 8 minutes in inert atmosphere of argon gas. The as-cast specimens were then heat-treated (T6) to the following schedule: 8 h at 520 °C, followed by water quenching (25 °C) and artificially aging for 8 h at 180 °C. Tensile results reveal that nanocomposites show a different tensile

behavior compared with that of the microcomposites. Strength and stiffness increased with increasing content of reinforcement. However, with 1.5 vol. % TiB_2 nanoparticles significant improvement in tensile strength was observed. But with further increase in TiB_2 content reduction in strength values and elongation of nanocomposites which may be due to greater agglomeration of particles and higher degree of porosity. The highest toughness and total strain are observed in the 1.5 vol. % TiB_2 nanoparticle reinforced composites. Also the composites fabricated at 750 °C and 800 °C show higher tensile strength compared with that of the same sample fabricated at 900 °C. Agglomeration of nanoparticles and individual microparticle was observed on dendrites in fracture surface of samples. Coarse, fine and ultra fine dimples were seen in vast areas of fracture surface of composites. One of the main mechanisms of fracture was Silicon cracking and debonding in A356 TiB_2 particle reinforced composite.

Balasubramanian and Maheswaran **[17]** investigated the mechanical resistance behavior of AA6063 particulate composites with the inclusion of micron-sized silicon carbide (SiC) particles with different weight percentages of 0, 5, 10, and 15 weight percent of SiC by stir casting process. The average grain size of 17–20 μm and it was preheated to 600 °C. The stirring was done for for 10–15 minutes at 600 rpm. By Vicker's hardness test average hardness value of 55.8, 64.17, 71.93 and 86.07 kgf/mm^2 for 0%, 5%, 10% and 15% of SiC content were obtained. By tensile test the average tensile strength values of 140.94, 165.97, 180.61 and 175.25 N/mm^2 for 0%, 5%, 10% and 15% inclusion of SiC were obtained respectively. The tensile strength value of the samples initially increases as the percentage of SiC increased up to 10% and then decreased for 15% SiC inclusion. Fractography images show that for 0%, 5%, 10% and 15% SiC inclusion in the composites a combination of brittle fracture and dimple ductile fracture was observed. But sample with 15% SiC inclusion revealed more brittle fracture due to an increase in initiation and growth brittle fracture cleavage facets as a result the tensile strength decreased.

Balaji et al. **[18]** fabricated composite of aluminium 7075 alloy with Silicon Carbide (SiC) as reinforcement by stir casting method. Preheating of particles was done and stirring was done at 400 rpm for 10 minutes. Melt was poured at temperature of 720 °C. Tensile test results show that Al7075-SiC composites exhibits higher tensile strength as compared to

Al6061-Al2O3 composites. Micrrohardness of the composites also increased with increase in reinforcement content. The increase in microhardness of Al7075-SiC composites was found to be around 10%.

Viswanath et al. **[19]** fabricated composite of AZ91 alloy reinforced with SiCp by stir casting process. Investigation on mechanical properties and creep behavior was done. At the temperature of 750 °C, stirring was carried out using a steel impeller at 750 rpm. Preheating of SiCp particles was done at 600 °C. Composites were prepared with varying percentages of SiCp i.e. 5, 10, 15, 20 and 25% by weight of the matrix. The stirring was continued for 10 min after complete addition of SiCp to ensure the mixing of reinforcement into the matrix. The creep test was done at a temperature of 175 °C under constant stress of 80, 100 and 120 MPa. Test results show that creep deformation increases with increase in stress and associated time decreases as the load elevates. Creep curves show reduction in minimum creep rate with decreasing the applied load. Tensile test results show gradual increase in Yield strength with increase in amount of reinforcement. This increase is limited to elastic region as UTS of the composites do not show considerable variation from that of base alloy. This may be due to porosity and agglomeration of particles. Fractography of the surfaces of the composites reveal both ductile and brittle mechanisms. The brittle fracture region increases with increase in SiCp.

Ravi et al. **[20]** used stir casting technique to fabricate Aluminium Matrix Composites (AA6061) reinforced with Boron Carbide (B_4C) having different weight percentages. The average size of reinforcement particles used was 25μm. During fabrication B_4C powder was heated to a temperature of 250 °C so as to remove the moisture. The stirring was done for 10-15 minutes at 400 rpm impeller speed at 800 °C. Composites with 5 and 10 wt. % B4C were produced. Addition of B4C reinforcement particles decreased the grain size of the matrix. Vickers hardness test was done at a load of 300g for 10 seconds on samples. The microhardness of the composite increased with increase in weight percentage of reinforcement. It increased from 62 HV to 68 HV. Test on Universal testing machine (UTM) also showed increase in tensile strength of Aluminium Metal Matrix Composites. The tensile strength increased from 117 MPa to 145 MPa.

Aravindan et al. **[21]** Magnesium alloy (AZ91D) composites reinforced with silicon carbide particles having different volume percentage. The process used was two step stir casting process. The effect of changes in volume fraction and size of particles was investigated on physical and mechanical properties of composite under as cast and heat treated (T6) conditions. Pure magnesium blocks (99.95% purity) along with 10% aluminium, 1% zinc and 0.4% manganese were heated in a microprocessor controlled electric resistance furnace under controlled atmosphere of inert gas (Argon). Silicon carbide particles with an average size of 32 mm and 105 mm were used as reinforcement. Their preheating was done and were added while stirring at 680 °C. Stirring was done for 15 minutes at 600 rpm. The melt temperature was brought down to 620 °C. It was then heated rapidly to 700 °C and then poured. Composites were subjected to solution hardening and artificial aging (T6) heat treatment. Hardness tests show that hardness increased with the increase in the volume percentage of SiC reinforcement particle irrespective of the size. It was due to presence of SiCp phase which restricts the localized matrix deformation during indentation and finer grain size of the composite. Hardness of the MMC reduced with the increased size of the SiC particle as smaller size reinforcement particle produce more dislocations in the composite. The heat treated composite exhibits higher hardness, than the as cast composites. Yield strength of the composites also increased with the increase in volume percentage of SiC particles. With increase in the volume percent more load can be transferred to the reinforcement which also resulted in higher yield strength. The strengthening effect of matrix is due to dislocation and precipitation hardening. The ultimate tensile strength of composite formed was observed to be less than Magnesium alloy (AZ91). Tensile strength is reduced by presence of any secondary hard phase. Same was the effect on ductility due to void nucleation in advance with increased amount of SiCp. Fractograph images show small voids & dimples at the fractured surface by which ductile mode of fracture can be predicted.

2.3.2 Fatigue, Wear and Impact behavior

Mahadevan et al. **[22]** investigated high cycle fatigue behavior of stir cast AA 6061-SiCp composites at room temperature with different volume fraction of particles (10, 15, 20,

25% reinforcement by weight). The testing of specimens was done under fully reversed cyclic deformation in the peak aged condition. The particles of average size of 23 microns were used. The specimens of composites produced were heat treated as per T6 condition. The stress amplitude vs. cycles to failure for the DRCs with varying reinforcement volume fractions was plotted. The results show that with increase in SiC particle fraction the fatigue strength also increased up to 20% reinforcement. But with 25% reinforcement the fatigue strength was lower than that of 20% reinforcement sample. This may be due to early crack nucleation. The plots also indicate towards ductility exhaustion. The plot of endurance limit (taken at 107 cycles) and percentage of SiCp reinforcement show that endurance limit increases with an increase in the percentage of reinforcement up to 20% but for 25% reinforcement sample there is reduction in the endurance limit due to clustering of particles. Fractograph images show two distinct fracture morphologies i.e. a propagation region and a fast fracture region. Except for composite with 25% reinforcement, Mode-I type of cracking (due to surface and sub-surface defects) was found to be the cause for crack initiation. The composite with 20% reinforcement had enhanced fatigue strength over others.

Gopalakrishnan and Murugan **[23]** did wear characterization of composite of Aluminium AA6061 with Titanium carbide fabricated by stir casting method. TiC in varying volume fraction of 3–7% was added to achieve good wettability. Wear test results show that wear rate marginally increases as the % addition of TiC increases and wear rate was lower when compared to pure aluminum. But the wear rate increases as the sliding velocity increases as at higher velocities temperature increases and thermal softening of matrix led to more wear rate. The wear rate increases steeply with the addition of normal force. It is because as normal load increases the coefficient of friction also increases due to which wear rate increase. Among these 3 parameters, sliding velocity had least effect on wear rate. Maximum wear rate of 53 _ 10_6 mm3/m was observed at 7% TiC (+1) and at a maximum load (+1) of 49.1 N.

Kumar et al. **[24]** studied the effect of dual reinforced particles (DRP) on high temperature tribological properties of aluminum composites. Composites with single (SRP) and dual reinforced particles (DRP) were made with commercial grade LM13 piston alloy with

Zircon sand and silicon carbide as reinforcement particles. The average size of particles used was 20–32 μm. Composites with DRP were made with 15 wt% reinforced particles by two step stir casting technique. Under dry sliding condition at high temperatures between 50 ºC and 300 ºC the wear behavior was studied. The stirring was done at 750 ºC at 630 rpm impeller speed. Particles were preheated at 450 ºC before mixing. The melt was solidified and then again re-melted and stirred for 12–15 minutes. Five different composites containing a total of 15 wt% reinforcement in different proportion of zircon sand and silicon carbide were fabricated. Wear tests show that a transition in the wear mode occurs after 150 ºC for all composites. The wear rate of both DRP and SRP composites decreases with increase in temperature from 50 ºC to 200 ºC at 1 kg load. At load of 5 kg wear rate increases slightly from 50 Cº to150 ºC andthendecreasesat200 ºC. Initially the alloy matrix expands and become soft compared to a later stage. However, the alloy gets strain hardened due to continuous sliding under an applied load after a certain sliding distance, which further offers resistance to wear and less loss is observed in between 50 ºC and150 ºC at higher load condition. Between 150 ºC and 200 ºC formation of oxide layer on the surface of pin protects the surface causing a decrease in wear rate as it prevents the direct metal-to-metal contact of sliding surfaces. It was found that the combination of zircon sand and silicon carbide particle in a ratio of (1:3) reinforcement in the composite exhibits better wear resistance as compared to other combinations at all the temperature at low and high load both. Also it was found that DRP's enhances the wear resistance as compared to SRP's if mixed in a definite proportion.

Sivananth et al. **[25]** evaluated the load bearing behavior of titanium carbide reinforced AMMC. Different volume fraction of reinforcement i.e. 10, 12 and 15, in the size of 325 meshes were fabricated by stir casting process. Mixing was done with a stirrer at a speed of 900 rpm and 800 ºC for about 10 minutes. Samples and steering knuckles were casted for testing. S–N curves were plotted after fatigue testing and they show that the fatigue strength increases with wt% of TiC. The MMC with 15 wt% TiC gave the highest fatigue strength of 248 MPa at 1E+07 cycles. Due to presence of TiC particles in the matrix high impact strength of Al–15 wt% TiC MMC was obtained which absorbed large amount of energy during impact testing. SEM images of fractured composite's surfaces show that the TiC particle began to crack in all directions around the particle due to sudden impact load.

This is due to strong interfacial bonding between matrix and the TiC particle. Also it was found that he unreinforced alloy allows the cracks to propagate rapidly in multiple directions without any obstacle and decreases the impact strength. The steering knuckle experiences load at four different locations. The steering knuckle fabricated was used in a passenger car of weight 1500 kg. The test results show Al–TiC knuckle with 15 wt% TiC withstands maximum ±5 kN load up to 1.80 E+ 06 cycles without any failure. The minimum load carrying capacity was for 10 wt% TiC knuckle. The fatigue test was successfully passed according to industrial testing standards. The graphs of load versus energy versus deflection for Al/TiC, SG iron and unreinforced alloy at an impact velocity of 4 m/s were prepared after impact tests. The crack initiation phase (linear) and crack propagation phase (constant) were seen but SG iron curve didn't show crack initiation and propagation zones. The results show that steering knuckle impact strength increases with the increase of TiC particulates weight percentage and one with 15 wt% TiC absorbed 670 Joules of energy with a deflection of 16 mm before fracture and impact load of 43 kN was required to initiate a crack.

Ibrahim et al. **[26]** prepared composites using two series of aluminum one was pure and other was AA6063 to investigate the impact toughness of the composites. Very small amounts of Ti, Zr and Sc were added to those composites, either combined or individually. B_4C was used as reinforcement with volume fraction of 12-15 vol. %. Ten MMCs were produced by powder injection technique. The stirring was done for 20 minutes at 300 rpm at the temperature of 730 °C. Charpy impact testing was performed on unnotched specimens. Test results show that pure aluminium based composites offered better toughness compared to those obtained from 6063/B4C composites. The toughness of composites was mainly controlled by precipitated phase amount. The precipitation of Mg_2Si in 6063/ B_4C was found to be more effective in controlling the composite toughness than Al_3Zr and/or Al_3Sc when the composite was aged at 200 °C. Overaging also improved the toughness. Cracks were always initiated at the particle/matrix interfaces and propagated either through the B_4C or along the protecting layer or both, depending upon the particle/matrix adhesion. The occurrence of complete debonding was prevented by presences of protecting layers rich in Zr and/or Sc.

2.4 MACHINING OF METAL MATRIX COMPOSITES

Manna,and Bhattacharayya **[27]** carried out an experimental investigation on the machinability of silicon carbide particulate aluminium metal matrix composite ($LM6Mg15SiC_p$) during turning using fixed rhombic tools. The influence of machining parameters, e.g. cutting speed, feed and depth of cut on the cutting force and surface finish criteria were investigated during the experimentation. Results indicate that cutting forces are more or less independent of cutting speed in range of 60 to 150 m/min. The flank wear rate is high at low cutting speed due to the generation of high cutting forces and formation of BUE during machining of Al/SiC-MMC.

Kılıckap et al. **[28]** investigated the tool wear and surface roughness of A356 homogenised 5 wt %SiC-p (average particle size 24 μm) aluminium MMC materials. Two types of K10 cutting tool (uncoated and TiN-coated) were used at different cutting speeds (50, 100 and 150 m/min), feed rates (0.1, 0.2 and 0.3 mm/rev) and depths of cut (0.5, 1 and 1.5 mm). In dry turning condition, tool wear was mainly affected by cutting speed. It increased with increasing cutting speed. Surface roughness is again mostly affected with cutting speed. Higher cutting speed produced better surface finish. Feed rate was an effective machining parameter on surface roughness. Higher feed rates produced poor surface quality. TiN - coated cutting tool provided better results. It decreased tool wear and provided smoother surface finish. Homogenized heat treatment affected material adversly, it increased tool wear and surface roughness.

Tamer et al. **[29]** produced rods of Al Si 7Mg2 material reinforced with 5, 10 and 15 wt % of SiC-p of particle size 30–60 μm were produced, 90 mm in diameter and 150 mm in length. TiN coated WC (K10) tool was used for turning. Machinability of MMC was very different from traditional materials because of abrasive reinforcement element. This was because abrasive element causes more wear on cutting tools. Flank wear of cutting tool had also increased with increase in reinforcement ratio. Influence of feed rate was not as effective as cutting speed on tool wear, but as the feed rate increased, the wear of cutting tool also increased. In turning of AlSi7 Mg2-MMC samples, surface quality improved

when cutting speed decreased. Surface roughness increased due to increasing feed rate values. It was found that increase in particle ratio affects roughness negatively.

Kannan et.al **[30]** took AA6061 and AA7075 as matrix material.10 and 15 vol % alumina particles were used as reinforcement material. Particle size was 9.5 µm, 20 µm and 25 µm. An experimental investigation was carried out to study the generated forces and the changes in the microstructure of the matrix as a result of cutting. The obtained data revealed that the forces generated during cutting of MMCs can be correlated to the average dislocation density in the matrix. This change in the microstructure, in terms of average dislocation density in the matrix, is due to the various mechanisms operating as a result of changes in the cutting conditions, material compositions and reinforcement volume fraction and sizes. It has been shown that the increase in the cutting force as a result of increasing the particle size and volume fraction can be correlated to the increase in the average dislocation density. In addition the amount of deformation in the matrix is dependent on the type of material matrix as well as the volume fraction and the average particle size.

Altınkok **[31]** fabricated composite of A332-Al2O3/SiCp by stir casting method and machinability properties were studied at different cutting conditions. The volume fraction of reinforcement used was 10 wt% and different average sizes of 2, 10, 20, 38, 45 and 53 µm. The mixing was done at 650 rpm at 700 ºC. Machining tests were carried out to determine the tool wear or tool life under various cutting conditions when cutting three types of composites and their alloy matrix. The tests were carried out on lathe machine without the use of coolant. Test results show that by increasing particle size, tool wears decreases at low cutting speeds; when values of feed rate and cutting depth are constant. The tools wear increases with cutting speed. The lowest surface roughness has been found in 53 µm Al_2O_3/SiCp reinforced composite materials and the highest wear is seen in 2 µm particle reinforced composite, at constant cutting speeds and feed rates. Also it was reported that with increase in cutting speed the tool wear increased. Also by keeping cutting speed and depth of cut as constant and increasing the feed rate, the surface roughness was determined. At constant feed rates flank wear of cutting tool increased with the increase in particle size. Surface roughness increased due to increasing feed rate values. And the decrease in size of particles affected the roughness negatively. Also the analysis of

chips was done which revealed that the length of chip and the number of chip curls increases with an increase in feed rate at given cutting speed and depth of cut. Also the chip formation mechanism was influenced by the size of reinforcement considerably. The chip segments were longer in length and gross fracture occurred at outer surface of the chips only in case of coarser reinforcement composites whereas in case of finer reinforcement composites, complete gross fracture caused the formation of smaller chip segments.

2.5 Research Gap

On the thorough scrutiny of the published work on the aluminium alloy for light weight applications, the following observations have been made:

- There is no information available in the direction of optimization of percentage of alloying elements.
- Literature lacks in furnishing the consistent and sufficient theory about the machinabilty of various developed aluminium alloys.
- There are conflicting opinions from various researchers regarding the effect of some of the elements on the properties of the alloy.
- Optimization of process parameters during machining of 7075 Al alloy B_4C and SiC composites has not been studied.

Although a lot of efforts have been directed towards the development of aluminium metal matrix composites for light weight applications, yet several key issues (e.g. impact of addition of rare earth metals, properties of alloys at elevated temperatures, optimization of elements for alloy, machinabilty of the alloy etc) remain mostly untouched.

2.6 Objective of the work done

After thorough studying of various papers and keeping in mind the research gaps as well as the other boundations following objectives were set:

- Design and development of set up for Stir Casting Process.
- Development of Aluminium metal matrix composite (AMMC) by SCP.

- Characterization of developed AMMC along with mechanical testing.
- Machinability study of developed AMMC using DOE.

2.7 Research Plan

After studying and analyzing various research papers and taking expert guidance I intend to do the following for my research work:

- To fabricate Aluminium alloy composite by Stir casting method having B_4C i.e. Boron Carbide as reinforcement and Aluminium alloy AA7075 as matrix. Also to produce as-casted Aluminium (AA7075) alloy.
- Characterization of developed AMMC and as-casted Aluminium (AA7075) alloy which include optical micrography, SEM, XRD.
- Perform various tests on the specimen fabricated as well as of as-casted Aluminium (AA7075) alloy and determine its mechanical properties such as tensile strength, hardness and percentage elongations. To study its wear behavior etc.
- To carry out machining of developed composite using Design of Experiments (DOE) by varying speed, feed and depth of cut.
- Comparing the results with the results of other alloys and composites that are currently being used in the industry.

CHAPTER-3

EXPERIMENTAL SET UP DEVELOPMENT AND TESTING

This chapter includes information about set-up of stir casting, process of fabrication and techniques for characterization of as-casted 7075 Al alloy and AA7075/5 wt % B_4C composite.

3.1 Experimental set-up

The set up of stir casting furnace was installed in 'Precision manufacturing lab.' The set up consists of 2 main parts namely:

I. **Bottom loading furnace** which has following specifications :

- Working temperature-1400°C
- Maximum temperature-1500°C
- Heating elements- Silicon carbide heating elements placed on two sides.
- High density ceramic insulation.
- Bottom lid closed by motorized lifting.
- Melting capacity- 2-3 kg.

II. **Temperature control panel** with specifications as :

- Control panel : Placed on the side of furnace with all components

- Temperature programmer: PID programmer having minimum 1prog with 1 segments (ramp/soak)
- Stirrer : Variable speed stirrer
- Power control : SCR Unit (phase angle thyristor)
- Power supply : 220 volts single phase 50 Hz

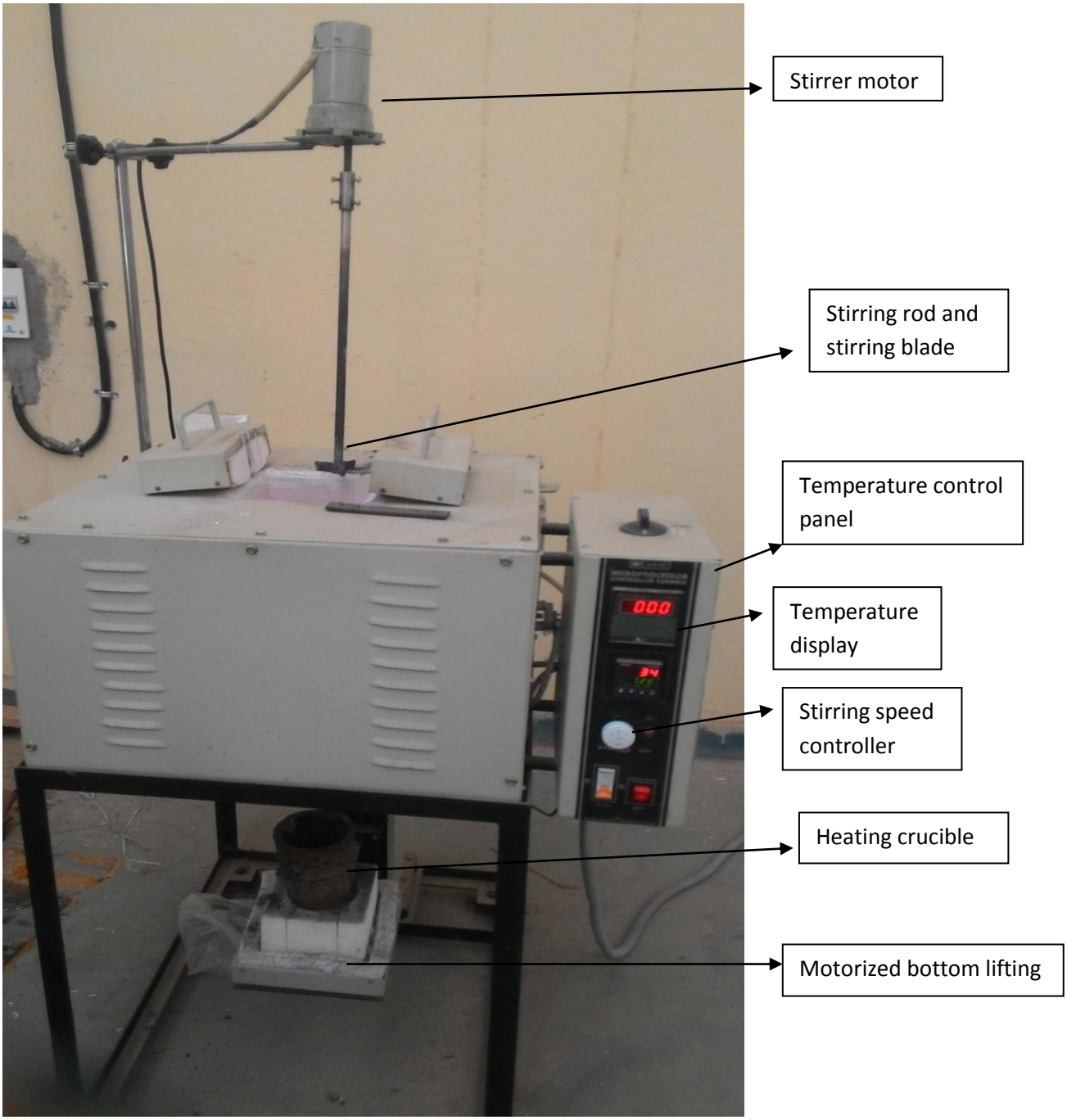

Figure 3.1: Experimental set up for Stir casting of Aluminium.

3.2 MATERIALS

The aluminium alloy AA7075 and B_4C ceramic powder (Mesh size of 400 or average size of particles 37 μm) were chosen as raw materials for matrix phase and dispersed phase respectively.

Table 3.1 Chemical composition (wt %) of 7075 Al alloy

Material	Zn	Mg	Cu	Cr	Si	Fe	Al
Wt %	5.65	2.34	1.79	0.182	0.079	0.177	balance

The following castings were obtained from these raw materials:

- AA7075/0 wt % B_4C Particles (37 μm).
- AA7075/5 wt % B_4C Particles (37 μm).

3.3 Fabrication of Aluminium Alloy-SiC Composites.

The composite was prepared using the set-up of Stir casting as shown in Figure 3.1. The various steps which were involved in making the AA7075/B_4C composite by stir casting process are as follows:

- Melting of the matrix material i.e. AA7075.
- Pre-heating of the reinforcement material.
- Mixing of the reinforcement particles.
- Casting of the composites.

3.3.1 Step 1-Casting of the composites.

800 grams of commercially available AA7075 aluminium ingots were placed the silicon carbide crucible which was then placed in the chamber of stir casting set-up. The

temperature of furnace was set at 710 ºC. The heating was continued for 2 hours during which the alloy melted.

3.3.2 Step 2-Pre-heating of the reinforcement material.

Because of very small size of B_4C powder in solid-phase, it does not mix well with liquid-phase of AA7075 due to difference in density and surface energy of two materials. Therefore the reinforcement particles were preheated to a temperature of 200 ºC in the heating furnace for 2 hours.

3.3.3 Step 3- Mixing of the reinforcement particles.

After melting of AA7075 aluminum alloy the temperature of liquid matrix was raised to 755 ºC as the problem of wettability minimizes at high temperature. The stirring was started at 200 rpm and a vortex was formed in the crucible placed inside the furnace. Preheated B_4C particles in amount of 0% and 5% weight were added to molten matrix at the sides of vortex. The stirring was continued for 8-10 minutes.

3.3.4 Step 4- Casting of the composites.

The molten mixture was then poured into a permanent metallic mould of mild steel at the temperature of 755 ºC. The graphite sheets were inserted along the inner walls of mould so as to prevent the sticking of molten material with the mould material. The molten composite was allowed to solidify at room temperature.

3.4 CHARACTERIZATION OF MMC

Characterization of AA7075/0 wt% B_4C and of AA7075/5 wt% B_4C (average particle size 37 μm) was done by carrying out the following tests.

- **Scanning Electron Microscopy (SEM)**

  The samples were examined using scanning electron microscopy (SEM) HITACHI S-3700N. The samples were cut using hand hacksaw and samples were taken from different locations of the casted composite. The samples were then

finished using Emery paper from grade 220-1200 (220, 320, 600, 800, 1000, 1200) after which they were wet polished using alumina powder with water.

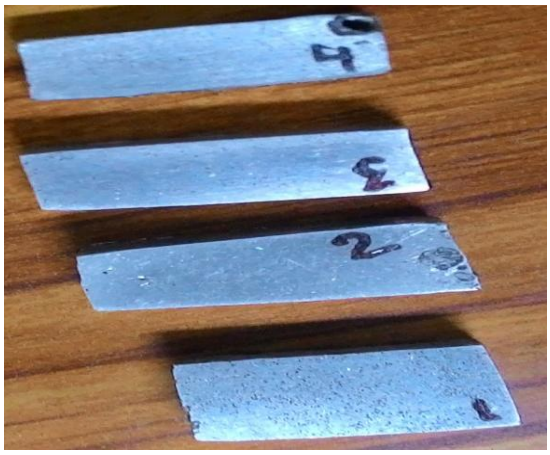

Figure 3.2: Samples for SEM and XRD analysis.

- **Optical Microscopy**

  The microstructure of samples was studied using OLYMPUS GX41 optical microscope. For studying the microstructure the samples were mounted for proper holding and then surface finished using Emery paper from grade 220-1200 (220, 320, 600, 800, 1000, and 1200) followed by wet polishing with alumina powder and water. After this the etching of the samples was done. The etchant used was Keller's reagent (2ml HF (48%) + 3ml HCl + 5ml HNO3 + 190ml H2O). This etchant gives the possibility to reveal grain boundary contrast and precipitates in several aluminium alloys and composites. After etching the surfaces were cleaned with de-mineralised water and dried. After that the samples were examined under microscope at different magnifactions.

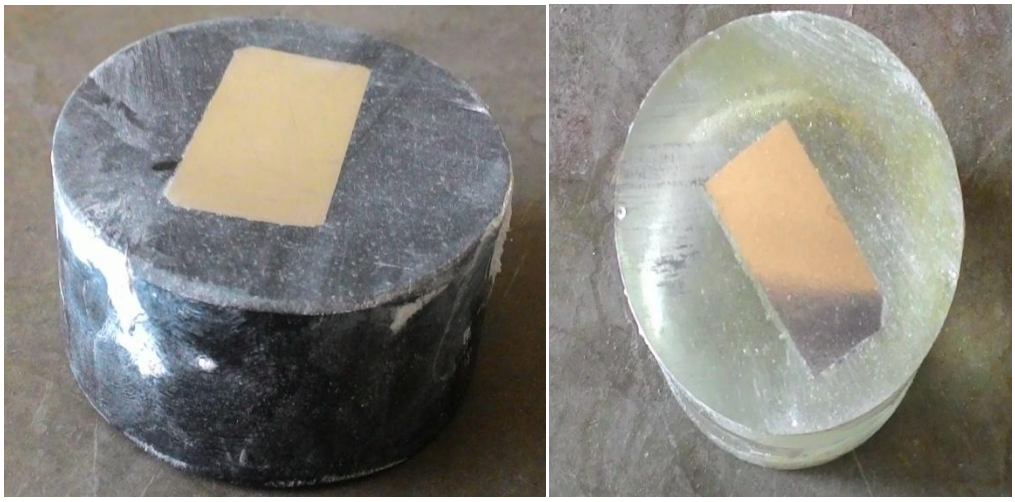

(a) **(b)**

Figure 3.3: (a) and (b) show different mounted samples for optical microscopy and Vickers hardness.

- **X-Ray Diffraction Analysis (XRD)**

  X-Ray Diffraction Analysis (XRD) was performed using BRUKER D8 Advanced X-Ray Diffractometer. XRD was carried out at a scanning rate of 0.01º 2θ/sec using Cu k (α) radiation. The source voltage and current were maintained at 40 kV and 40 mA. Peaks obtained in the diagram were analyzed.

- **MICROHARDNESS (Vicker's)**

  Microhardness of the samples was calculated on HV1 scale with diamond indenter. The load of 1kg was applied on samples with a dwell time of 10 seconds. Average of three readings was taken to obtain the final value of hardness. The samples used for microstructure study were used to carry out the testing for microhardness.

- **TENSILE TESTING**

  Tensile testing of the specimens was carried out and results for Ultimate tensile strength (UTS), Yield strength and % Elongation were obtained. The tests were

carried out according to standard IS : 1608-2011/ ASTM A-370. The specimens were obtained from casted samples with help of Wire EDM. The dimensions of samples used are as shown in figure 3.4.

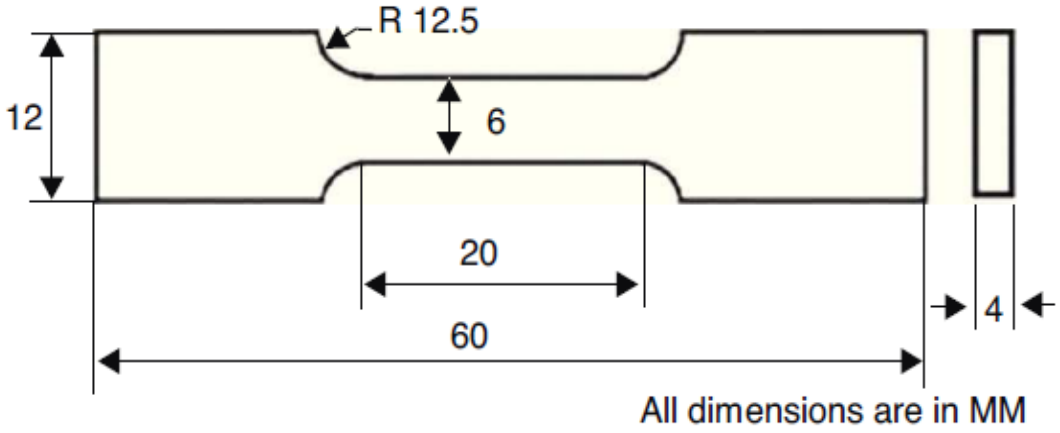

Figure 3.4: Schematic of Tensile specimen.

Figure 3.5: Tensile specimens obtained by Wire EDM cut.

- **WEAR CHARACTERIZATION**

The wear test was conducted on a pin on disc apparatus.

Test Procedure

1. For the pin-on-disk wear test, two specimens are required- a pin with a radiused tip and a flat circular disc.
2. The pin is positioned perpendicular to the circular disk.
3. The test machine causes either the disk specimen or the pin specimen to revolve about the disk center. In either case, the sliding path is a circle on the disk surface.
4. The plane of the disk may be oriented either horizontally or vertically.
5. The pin specimen is pressed against the disk at a specified load usually by means of an arm or lever and attached weights. Other loading methods have been used, such as, hydraulic or pneumatic.
6. Wear results are reported as volume loss in cubic millimeters for the pin and the disk separately.

Standard Dimension

The test specimen is in the form of a cylindrical pin with a hemispherical tip. The specimen was prepared on CNC lathe by Turning operation.

The test specimen was prepared in accordance with ASTM G99 standards. The specifications of the pin based on standards have been tabulated in the Table 3.2.

Table 3.2: Test Specifications Based On ASTM G99 Standards

Pin Size	12 mm
Wear Disc Diameter	165 mm
Wear Disc Thickness	8 mm
Wear Track Diameter	80 mm
Length Of Specimen	30 mm
Load On Pin	5 N
Disc Rotation	200 rpm
Temperature	40 C
Lever Length	400 mm
Test Time	20 min

Figure 3.6: Pin prepared for wear testing.

- **MACHINING OF COMPOSITE**

Turning of composite was carried out using Response Surface Methodology for optimization and software used for purpose was 'Design Expert'. A total of twenty experiments were carried out by varying speed, feed and depth of cut at five different levels.

Response surface methodology is a collection of mathematical and statistical technique useful for analyzing problems in which several independent parameters influence a dependent variable or response, and the goal is to optimize the response. Here RSM has been applied to study the effect of various parameters on the resultant force during turning operation.

At first the cubical shape casting was turned on 4-jaw chuck lathe in order to obtain the cylindrical workpiece. After that the machining of samples was carried out according to the table obtained by using Design expert and varying speed, feed and depth of cut. Various forces were measured using the dynamometer i.e. Cutting force, Feed force and Thrust force. The speed was varied in rpm, feed in inches/rev. and depth of cut in mm. Using these forces the Resultant force was calculated using the concept of merchant circle. The machining analysis was done

with resultant force as the factor. Here the influence of speed, feed rate and depth of cut on resultant force has been investigated.

Figure 3.7: Cylindrical specimens used for turning operation.

CHAPTER-4

RESULTS AND DISCUSSION

In this chapter results obtained after different testing and characterization have been discussed. Results have been supported by facts from literature available. Proper expert guidance was taken while discussing the results.

4.1 EVALUATION OF MICROSTRUCTURE

The optical micrographs of the composite obtained and that of the as-casted sample at different magnification have been shown in the figure 4.1, 4.2, 4.3 and 4.4.

The images show uniform distribution of B_4C particles in the AA7075 matrix. This may be due to effective stirring in the liquid state and also due to good wettability of reinforcement particles by melt of aluminium alloy.

Also it can be clearly seen that reinforcement particles are majorly present along the grain boundaries. The reduction in grain size has also been observed i.e. grain growth has been prevented by the addition of reinforcement particles. The number of nucleation sites gets increased by the addition of reinforcement particles into the matrix, by providing additional substrate during solidification and thus the grain size gets decreased **[20].**

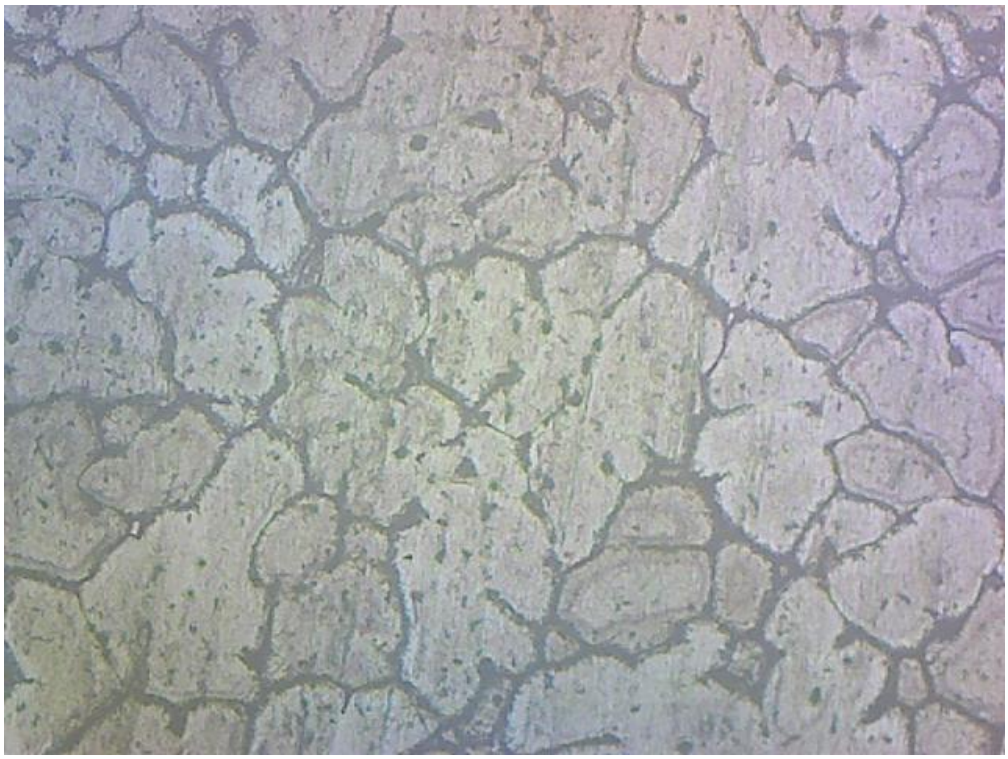

Figure 4.1: Microstructure of AMMC sample with B_4C at 100X magnification.

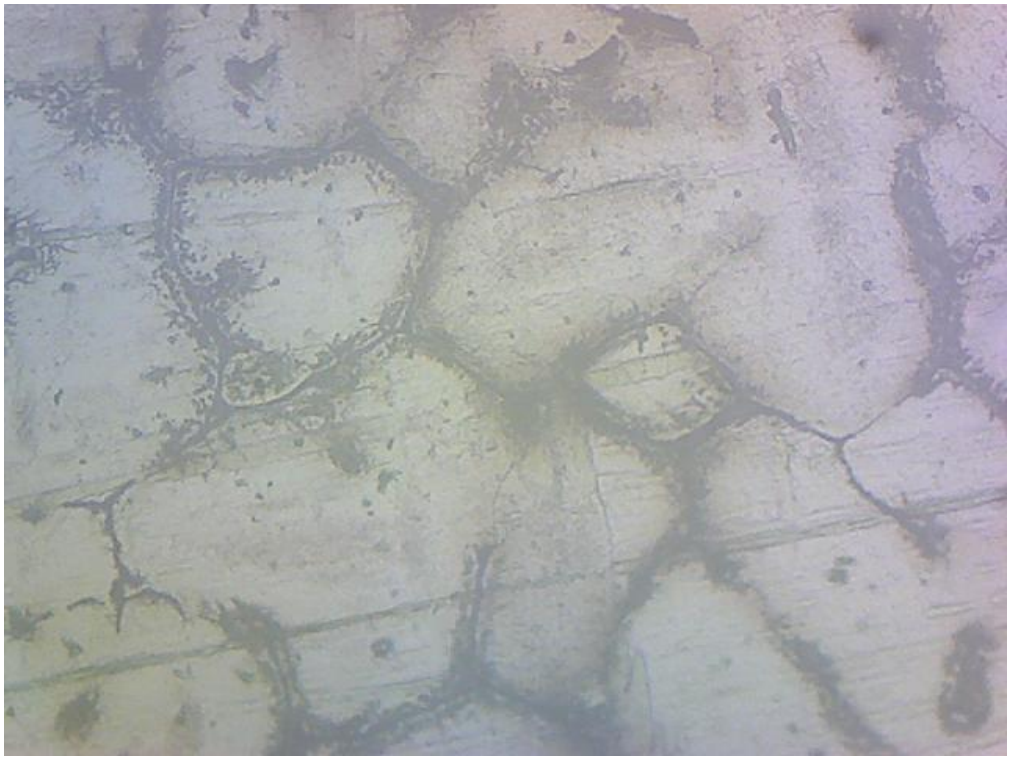

Figure 4.2: Microstructure of AMMC sample with B_4C at 200X magnification.

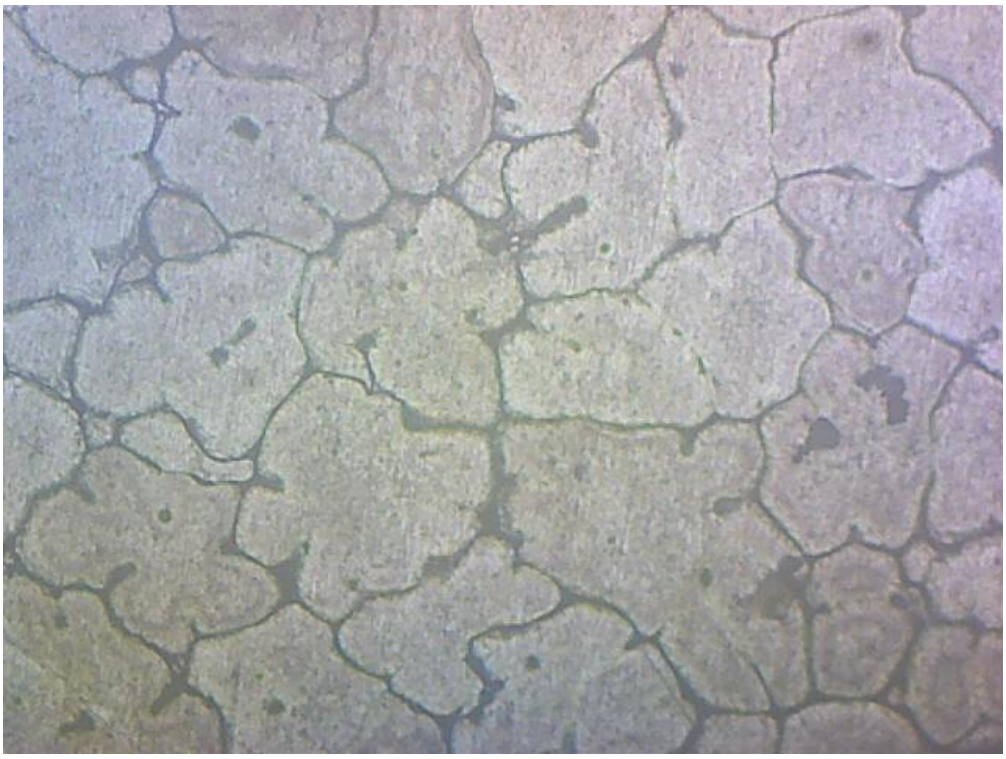

Figure 4.3: Microstructure of as-casted AA7075 sample at 100X magnification.

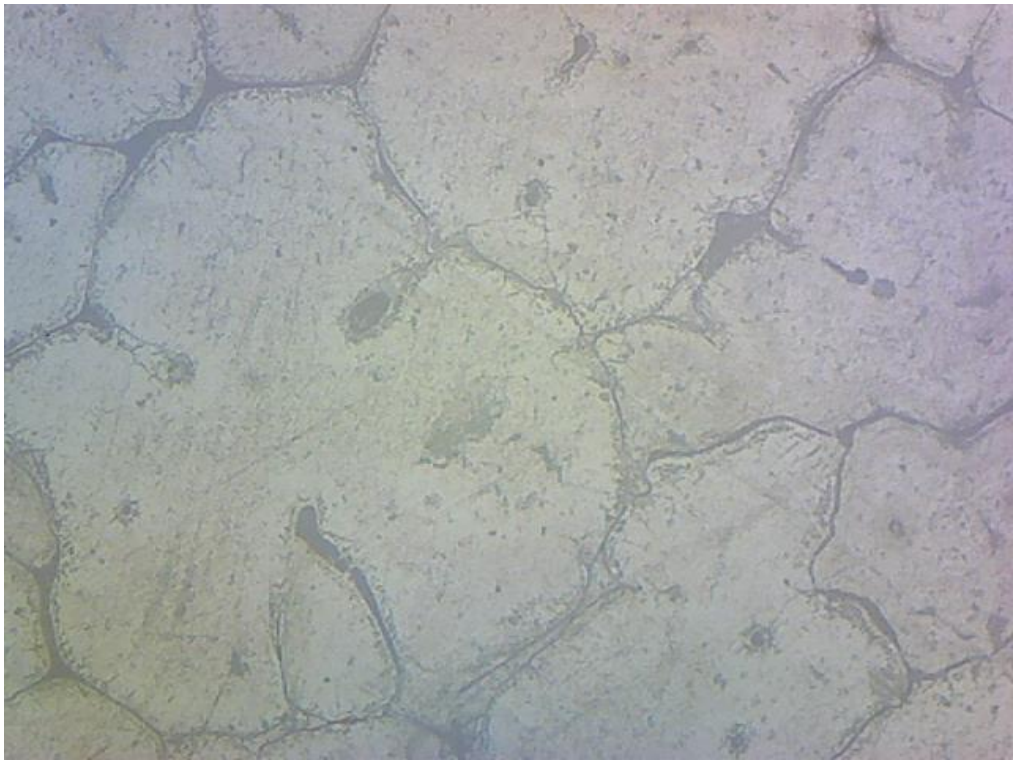

Figure 4.4: Microstructure of as-casted AA7075 sample at 200X magnification.

The uniform distribution of particles is further confirmed by SEM images as shown below in figure 4.6. Comparing figure 4.6 with 4.7 the presence of B_4C particles can be clearly observed in white shade. These may be Al-B particles and some others Al-C.

Both optical microscope as well as SEM images shows presence of micro porosity in the region of inter-grains. This could be due to entrapment of gases during casting. By addition of nano particles porosity volume percent has increased. Also the porosity increases with increasing time and stirring speed due to the effect of turbulence on increase of gas bubbles. Also micro porosity could be due to incomplete wettability **[9]**. In contrast to SiC reinforced MMCs the addition of B_4C particles has not that much associated with the formation of micro porosity **[26].**

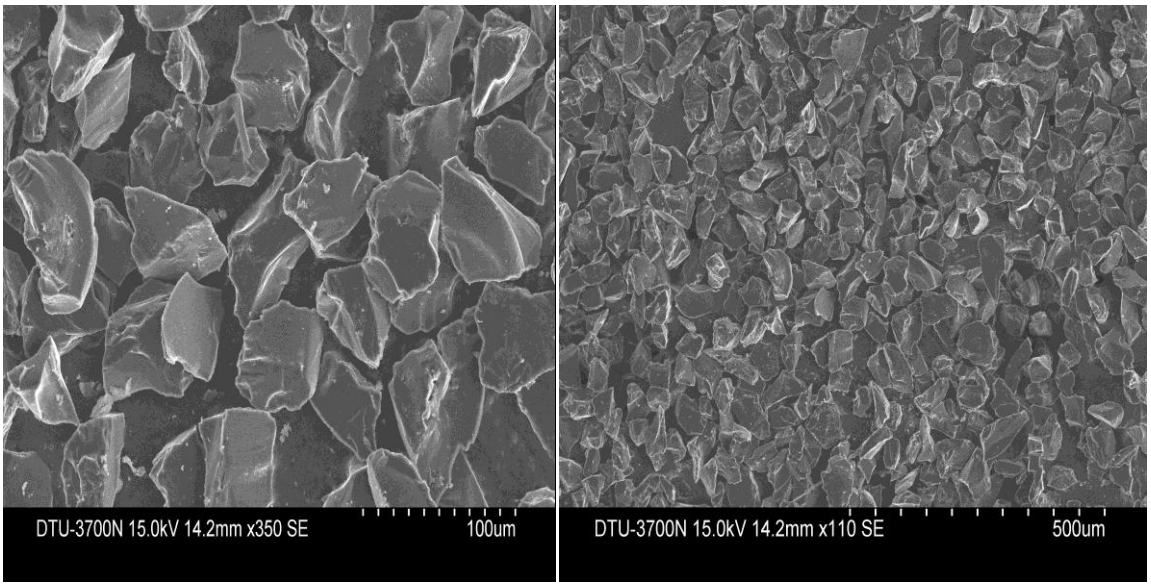

Figure 4.5: SEM images of B_4C powder at different resolutions.

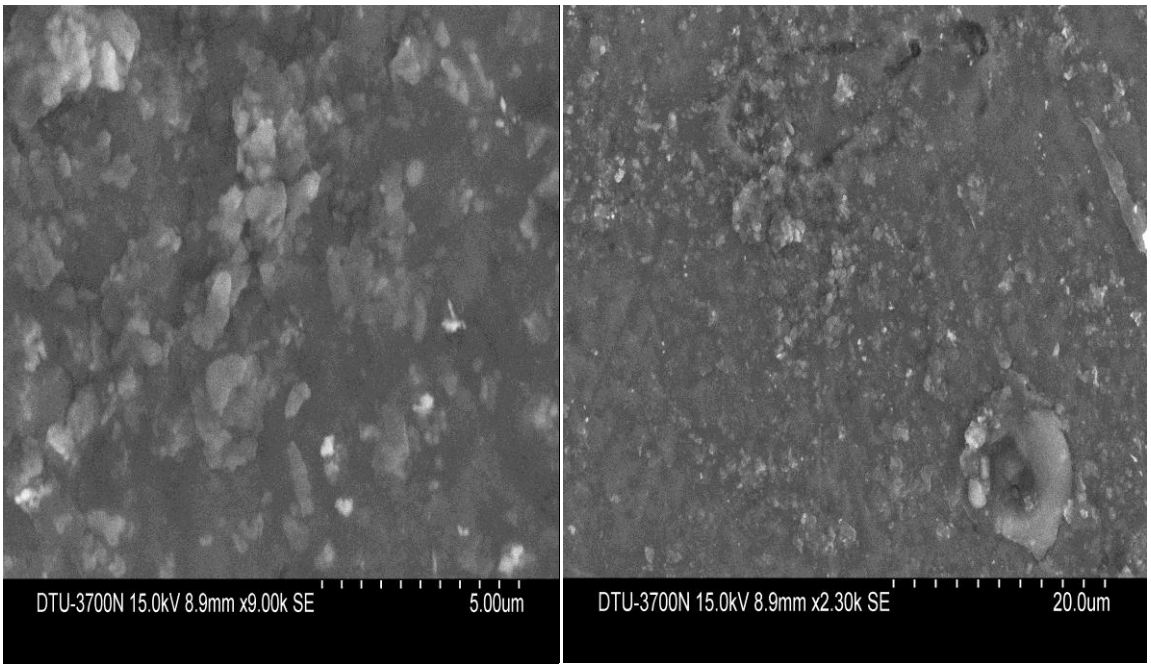

Figure 4.6: SEM images of AMMC with B_4C at different resolutions.

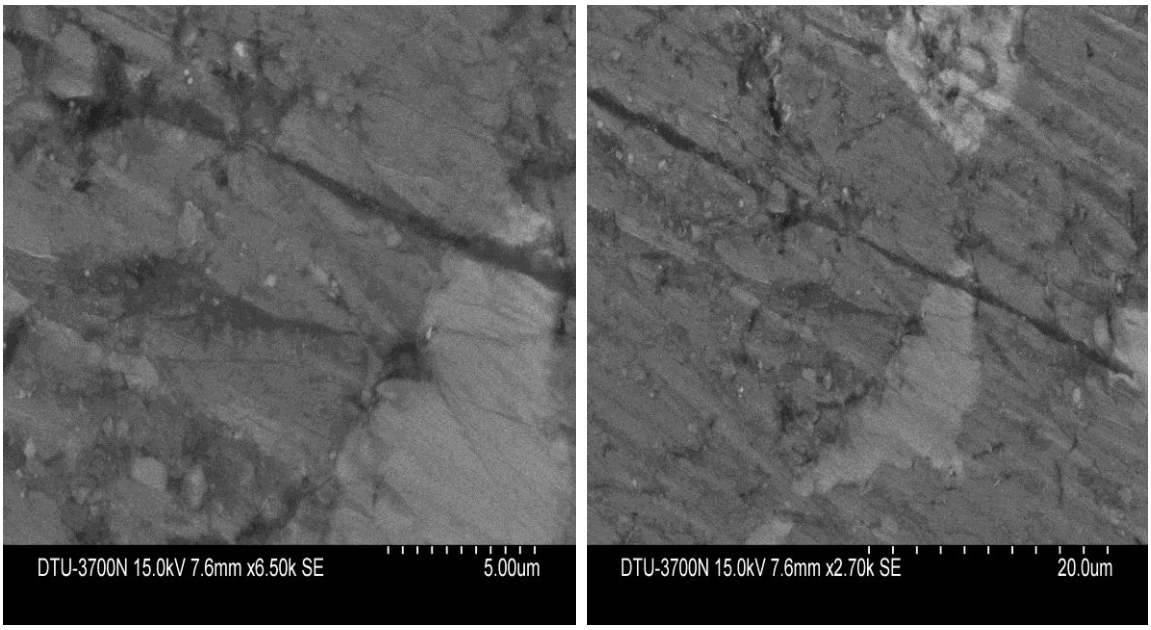

Figure 4.7: SEM images of as-casted AA7075 sample at different resolutions.

Also very few agglomerations have also been observed in the images. Generally, increase in agglomeration in composites is observed with high volume fraction of particle content. And it is also due to fine particle size as well as variations in parameters like stirring time, stirring temperature, stirring speed, etc **[19]**.

The analysis of XRD results was done using 'Match' software. The analysis confirms formation of compounds of boron with aluminum and magnesium. There are various peaks that can be observed but major peaks are as shown in figure 4.8.

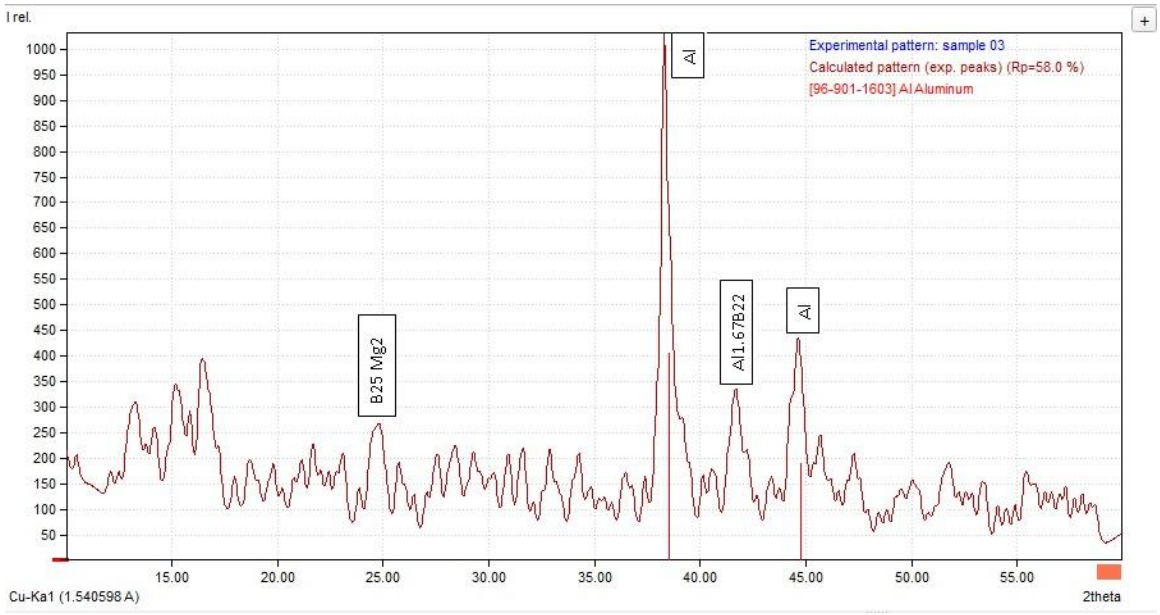

Figure 4.8: XRD pattern of developed AMC showing various peaks.

The major peaks are at 24.86, 38.30, 41.71 and 48.58. During the analysis at two of these major peaks were reported two main phases that were formed namely B25Mg2 (Dimagnesium pentaeicosaboride) and Al1.67B22. Complete XRD analysis confirmed the presence of compounds of Zn, Si, Fe and Cr but they were in very small amount.

4.2 MICROHARDNESS

The test results show an increase in hardness for the composite sample as compared to as-casted sample. The Vicker's hardness at 1kg load and dwell time of 10 seconds came out to be 110 HV and 101 HV for AA7075/5 wt % B_4C sample and AA7075/0 wt % B_4C sample respectively. The hardness increased by 9% approximately. The hardness value has increased due to presence of B_4C particles, as they are hard in nature and presence of hard particles on the surface resists the plastic deformation of the material. Due to the presence of hard phase an increase in strength of grain boundaries and decrease in dislocation of atoms is observed and thereby matrix gets strength and composite's hardness is increased **[20].**

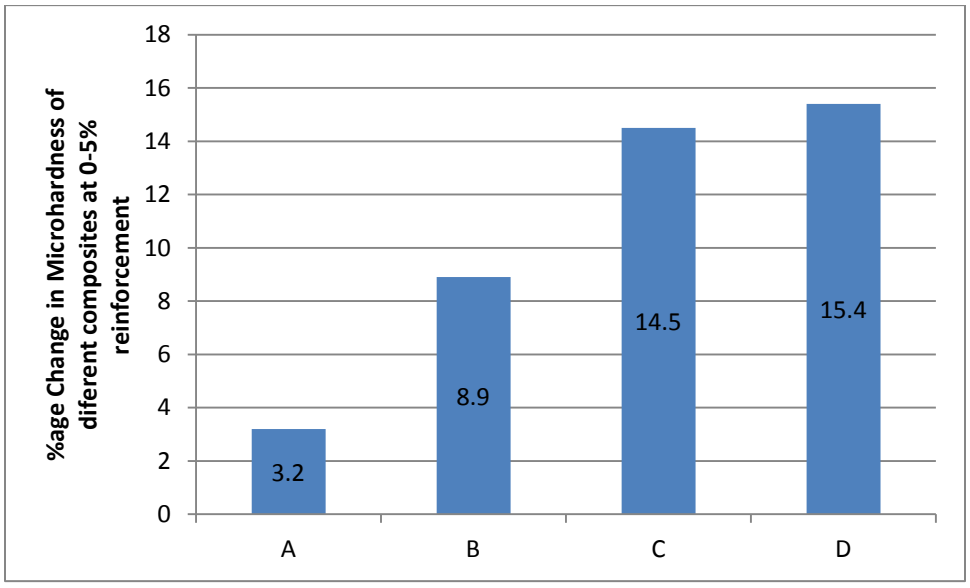

Figure 4.9: Comparison of %age change in microhardness of different composites with 5% of reinforcement particles.

- A- AA6061/5 wt % B_4C **[20]**
- B- AA7075/5 wt % B_4C **[Developed composite]**
- C- AA6063/5 wt % SiC **[17]**
- D- AA6061/5 wt % TiB_2 **[12]**

A comparison has been made with different Aluminium composites with 5% reinforcements. The data shows that AA7075/5 wt % B_4C composite has better hardness as compared to AA6061/5 wt % B_4C composite. This may be due to better alloying elements present in AA7075. However AA6061/5 wt % TiB_2 composite shows considerable improvement in hardness as compared to others which is due to better properties offered by TiB_2.

4.3 TENSILE PROPERTIES

The results show considerable improvement in Yield strength (YS) and Ultimate tensile strength (UTS) but the ductility decreased for the composite sample as compared to as-casted sample.

4.3.1 Yield strength

The Yield strength of the AA7075 has increased with the addition of reinforcement particles. The yield strength of composite came out to be 61.87 MPa as compared to 44 MPa of as-casted AA7075. The yield strength of the composite increased by approximately 40%. This strengthening effect in composites depends upon (a) Load-bearing effects due to the presence of reinforcement (b) Hall-Petch effect due to grain size refinement and the generation of geometrically necessary dislocations to accommodate thermal and elastic modulus mismatch between the matrix and reinforcements **[21]**.

From the figure 4.10 it can be seen that AZ91/5 wt % SiC_p composite shows considerable improvement in yield strength. This can be due to various factors like very less or negligible porosity, better grain refinement etc.

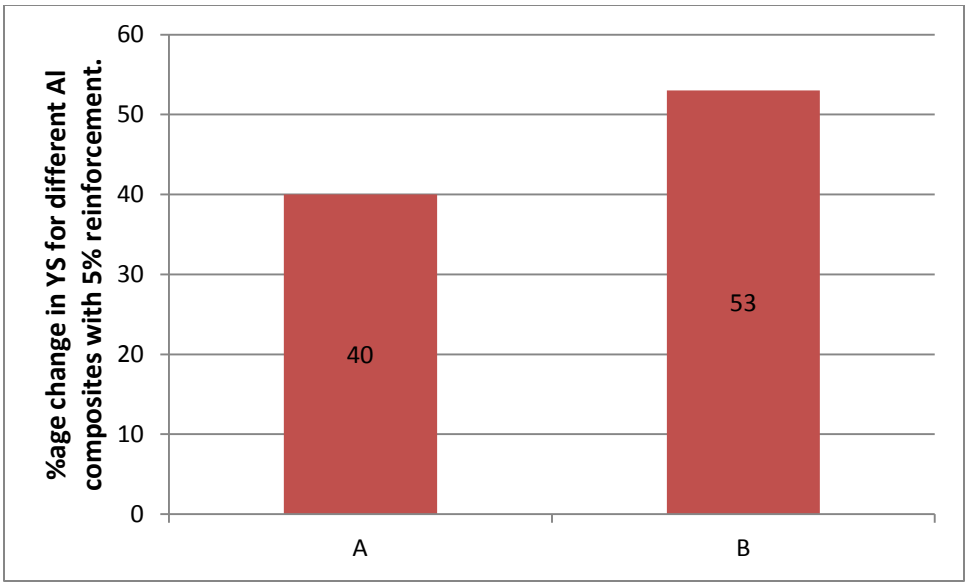

Figure 4.10: Comparison of %age change in YS for different Al composites with 5% reinforcement.

- A- AA7075/5 wt % B_4C **[Developed composite]**
- B- AZ91/5 wt % SiC_p **[19]**

4.3.2 Ultimate tensile strength

The ultimate tensile strength (UTS) showed an increasing trend. The UTS for the composite increased by 29% as compared to as-cast alloy. It is because stress is distributed to hard phase which delays the localized damage due to which tensile strength increases. Also when the composite is strained, the work hardening takes place and it generates a higher density of dislocations in the matrix which is around the reinforcement particles **[21]**. Also the hard phase of reinforcement restricts the flow of dislocations in the matrix **[19]**.

Due to large differences in the thermal expansion of metallic matrix and ceramic reinforcements during post fabrication heat treatment (like quenching) residual stresses are built-up which results in high dislocation densities near reinforcement particles or at the particulate/matrix interface resulting in enhanced dislocation density strengthening effect. This contributes in increasing tensile strength. But the porosity content and

clustering of particles can affect the load bearing capacity of matrix resulting in decrease of strength. And porosity could be due to less wettability of reinforcement particles by liquid phase of matrix. **[16]**

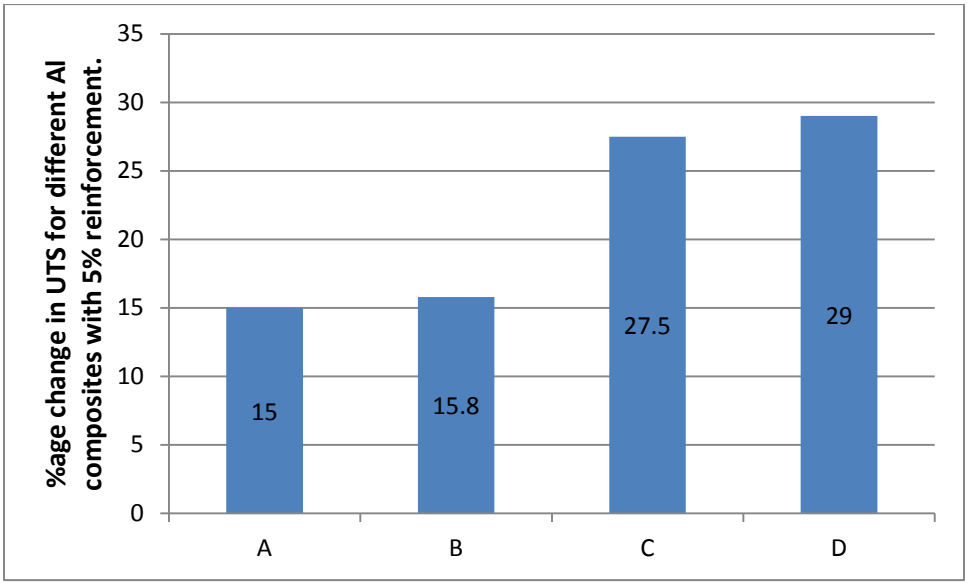

Figure 4.11: Comparison of %age change in UTS for different Al composites with 5% reinforcement.

- A- AA6063/5 wt % SiC **[17]**
- B- A356/5 vol.% micro - TiB2 **[16]**
- C- AA7075/5 wt% SiC **[18]**
- D- AA7075/5 wt % B_4C **[Developed composite]**

From the figure 4.11 it can be concluded that AA7075/5 wt % B_4C composite has shown good increase in UTS and this %age increase is close to AA7075/5 wt% SiC. This shows that AA7075 based composites possess better mechanical properties than most of other aluminium alloy based composites and it is because of presence of better alloying elements in it.

4.3.3 Ductility

Percentage elongation is the measure of ductility. And the tensile test results show a decrease in percentage elongation for AA7075 composite with B_4C as compared to the as-casted sample. The percentage elongation decreased from 2.67 % for as-casted sample to 1.40 % for the B_4C composite. It has generally been observed that ductility of the composite decreases with the introduction of hard reinforcement phase which may be due to increase in hardness and clustering of particles **[14]**. The addition of reinforcement phase probably overstrains the lattice and thus it no longer possesses enough strain energy to gain its ductility. Void nucleation might be another reason for the decrease in ductility for the composite material. **[21]**

4.4 Wear characterization

Following are the test results from wear testing:

Table 4.1: Wear Test conditions

Track Diameter(mm)	80
Disc rotation speed(RPM)	200
Load(gm)	500
Test Time(Minute)	20

Table 4.2: Weight of pins before and after wear testing.

	SPECIMEN	WEIGHT BEFORE TEST(gm)	WEIGHT AFTER TEST(gm)
Without Lubrication	AL7075-B_4C COMPOSITES	5.683	5.681
	AL7075 As Cast	5.670	5.669
With Lubrication	AL7075-B_4C COMPOSITES	5.681	5.681
	AL7075 As Cast	5.669	5.668

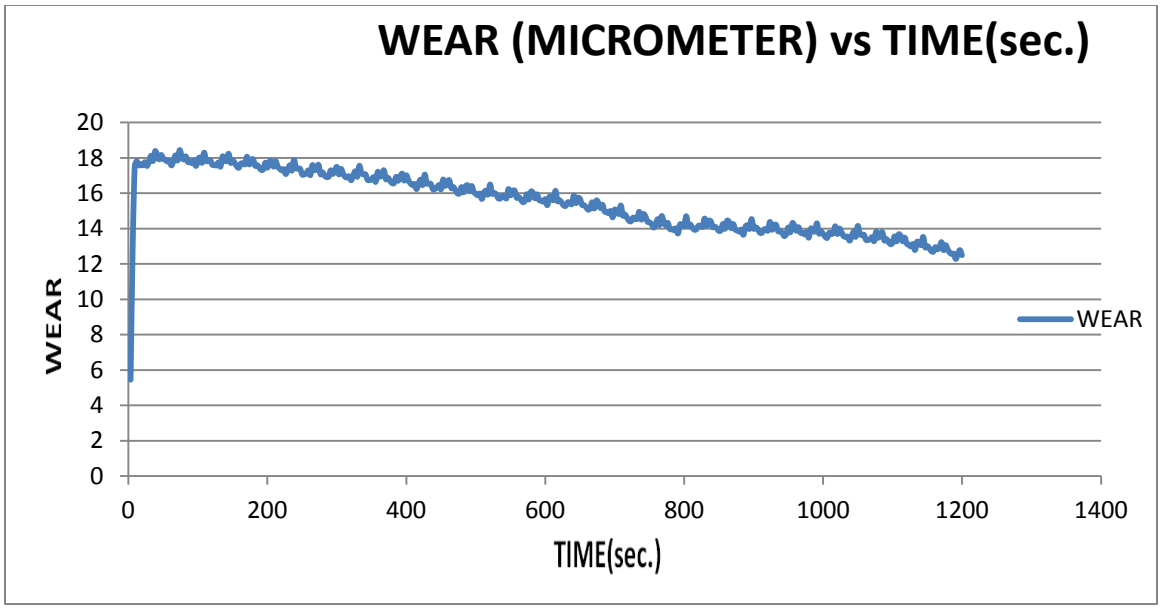

Figure 4.12: AA7075-B_4C composites wear observation with respect to time with lubrication.

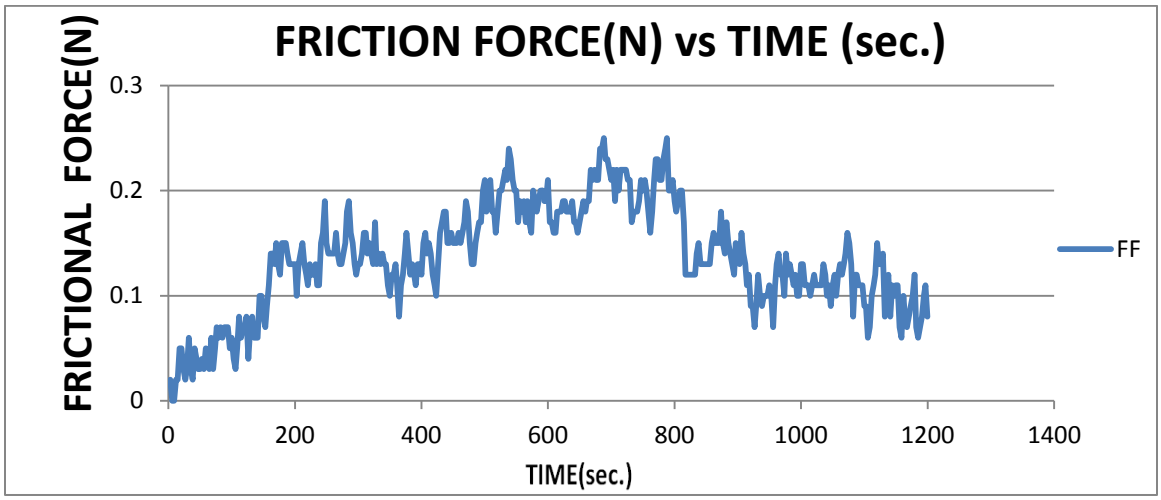

Figure 4.13: AA7075-B_4C composites friction force observation with respect to time with lubrication.

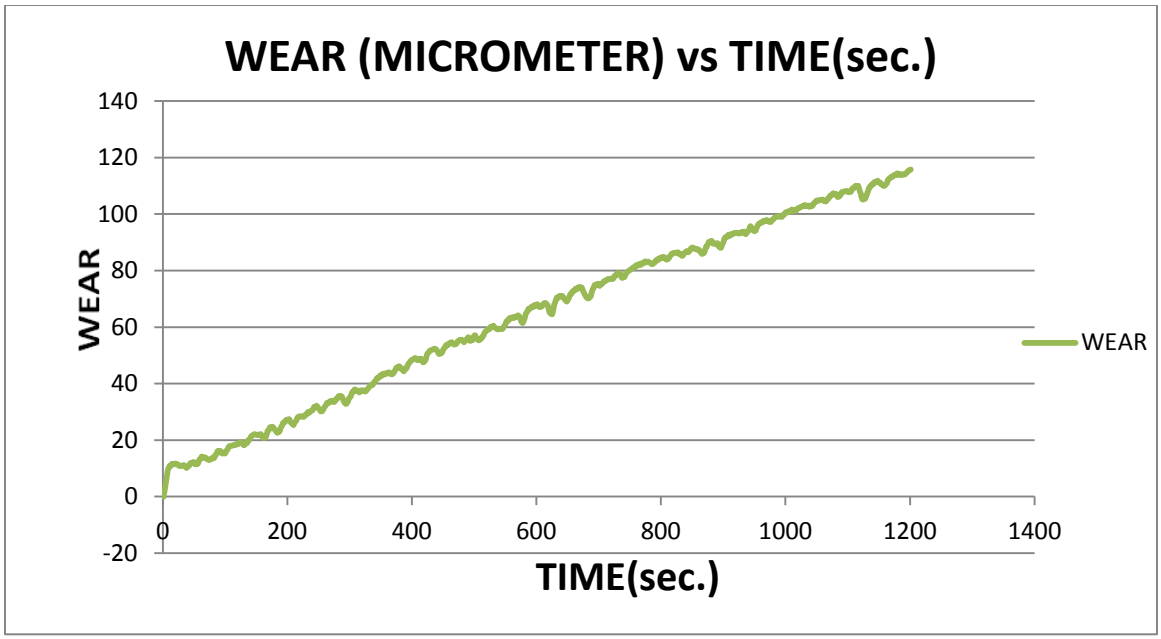

Figure 4.14: AA7075-B_4C composites wear observation with respect to time without lubrication.

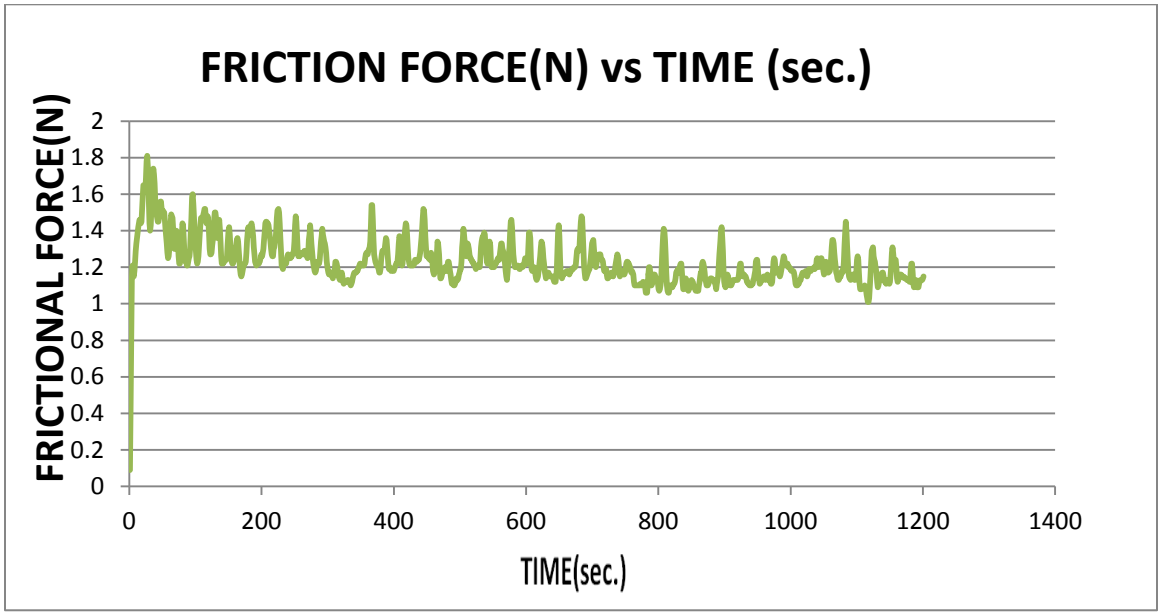

Figure 4.15: AA7075-B_4C composites friction force observation with respect to time without lubrication.

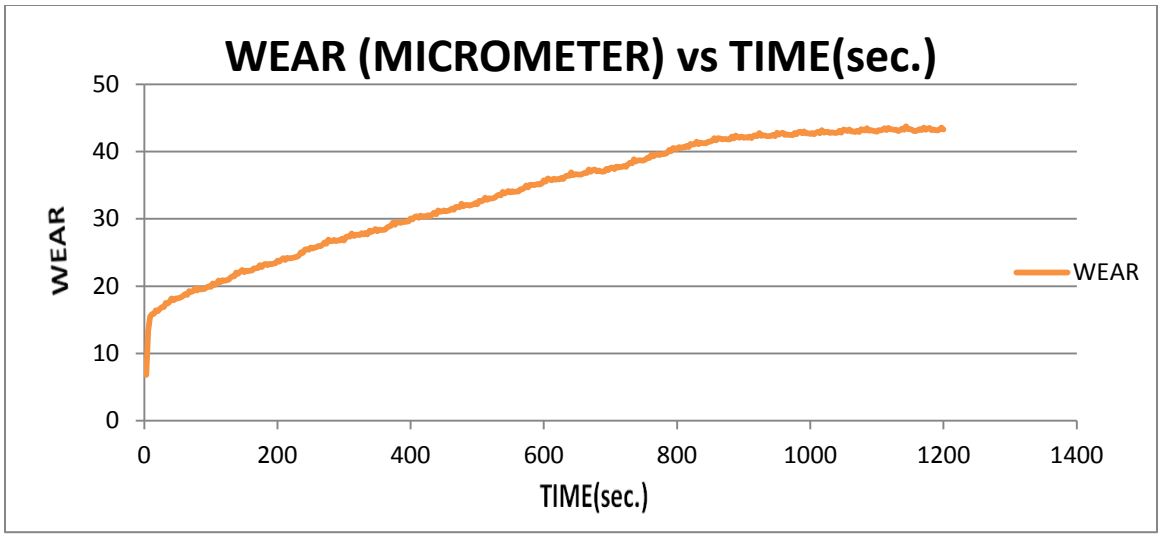

Figure 4.16: AA7075 wear observation with respect to time with lubrication.

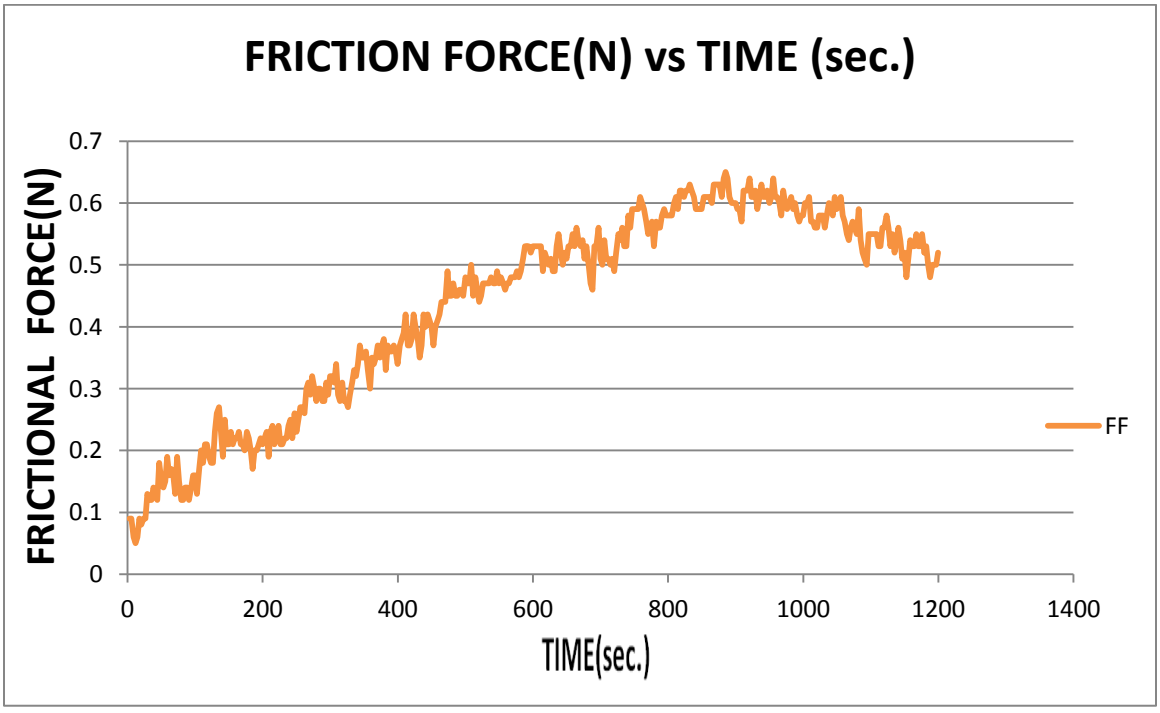

Figure 4.17: AA7075 friction force observation with respect to time with lubrication.

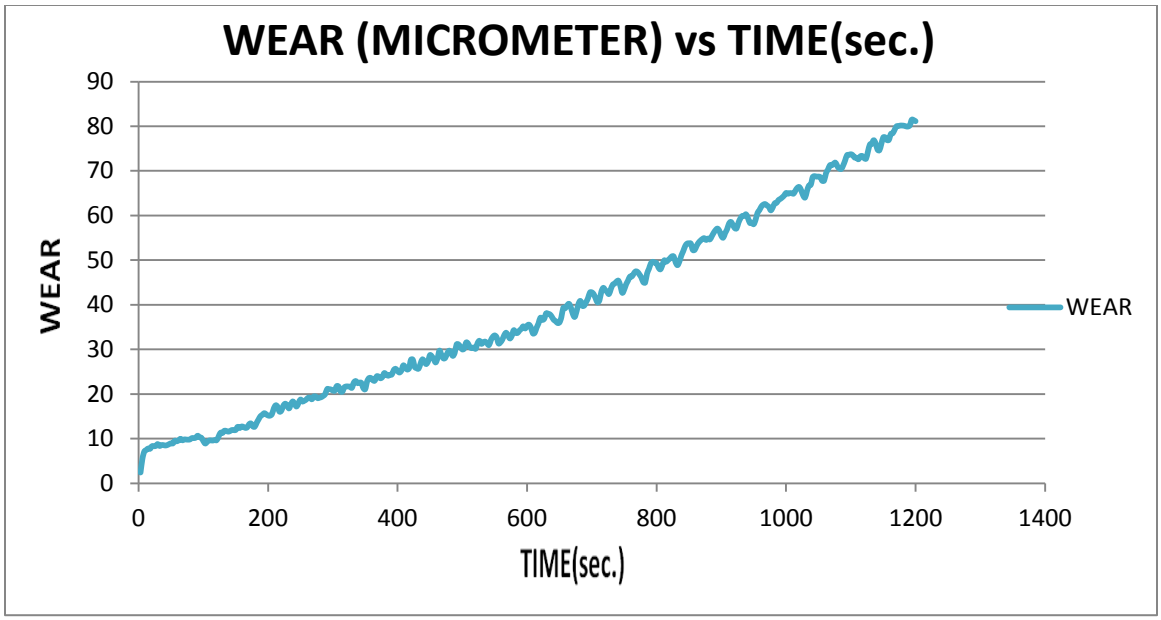

Figure 4.18: AA7075 wear observation with respect to time without lubrication.

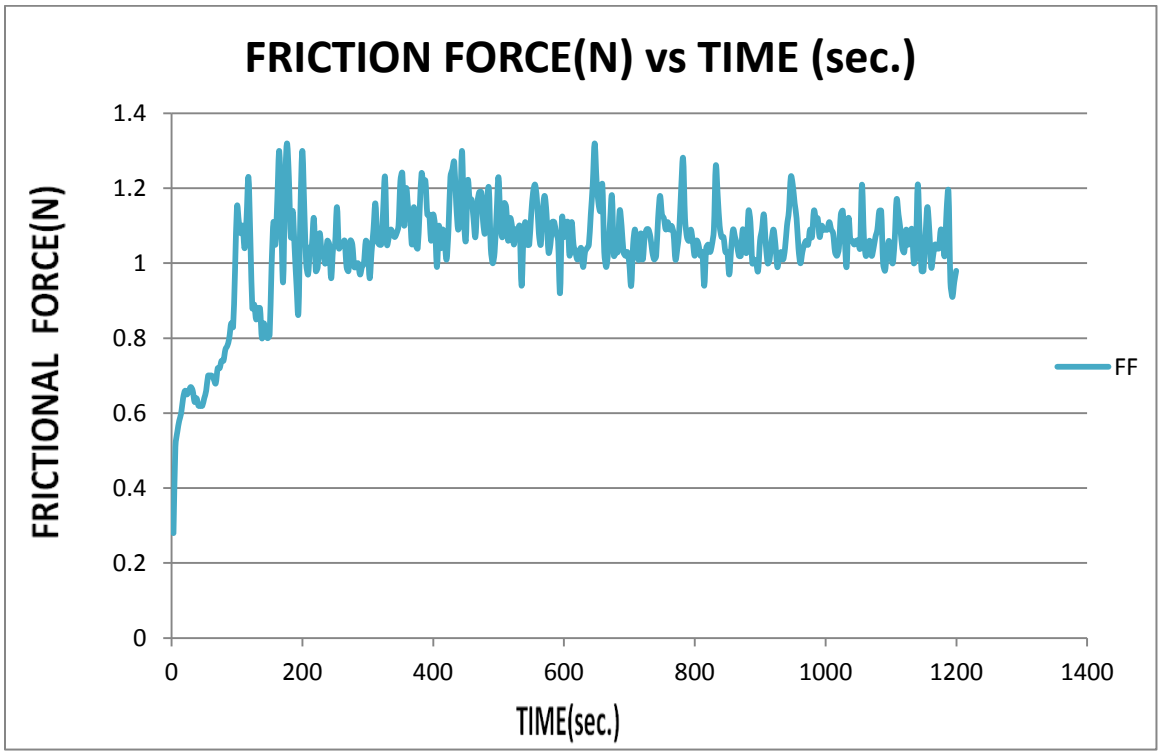

Figure 4.19: AA7075 friction force observation with respect to time without lubrication.

In a wear test employing constant operating parameters such as sliding force, applied load, and constant sliding distance, high-wear materials experience more material removal as microscopic chips due to micro-cutting while experiencing less material displacement in the form of micro-edges due to micro-ploughing. The variation in resistance behaviour of the composites due to inclusion of B_4C particles against sliding forces can be observed by the transition of wear mechanisms. The transition from micro-ploughing to micro-cutting is comparably less for specimens with B_4C as a constituent than without, and it has been concluded that the resistance of the material to sliding forces is increased due to the addition of B_4C particles.

Wear resistance increases with addition of boron carbide. This is in accordance with **[17]** where wear resistance increased due to addition of SiC.

Wear loss in terms of volume was for AMC as compared to Al 7075. Same was observed by **[23]** for Al–TiCp produced by in situ process.

4.5 Analysis of Machining

Resultant forces decide the ease of machining, less the resultant force more is ease of machining. Here the influence of speed, feed rate and depth of cut on resultant force has been investigated.

4.5.1 Analysis of machining for B_4C composite

The analysis was done by performing 20 set of experiments for which the set combination of process parameters was decided by using Design Expert. Table 4.3 shows the design matrix and results of experiments performed.

Table 4.3: Design matrix and Experimental results for B_4C composite using RSM.

		Factor 1	Factor 2	Factor 3	Response 1
Std	Run	A:Feed rate	B:Speed	C:Depth of cut	Resultant force
		inches/rev.	rpm	Mm	Newton
1	1	0.0025	156	0.3	13
2	2	0.0029	156	0.3	13.2
3	6	0.0025	409	0.3	13.4
4	9	0.0029	409	0.3	12.8
5	11	0.0025	156	0.7	24
6	19	0.0029	156	0.7	33
7	13	0.0025	409	0.7	17

8	14	0.0029	409	0.7	26.2
9	17	0.0023	282	0.5	16.8
10	3	0.0030	282	0.5	19.62
11	15	0.0027	69	0.5	28
12	7	0.0027	495	0.5	21.93
13	8	0.0027	282	0.16	13.87
14	20	0.0027	282	0.83	46
15	16	0.0027	282	0.5	15
16	5	0.0027	282	0.5	14
17	4	0.0027	282	0.5	13.4
18	10	0.0027	282	0.5	13.3
19	12	0.0027	282	0.5	16.1
20	18	0.0027	282	0.5	20

Values of "Prob > F" less than 0.0500 indicate model terms are significant. From table feed, speed, depth of cut and square term of depth of cut are significant model terms. Values greater than 0.1000 indicate the model terms are not significant. The final empirical relationship was constructed using only these coefficients, and the developed final empirical relationship is given below:

$R = +16.96 + 1.65*\text{Feed rate} - 1.76*\text{Speed} + 7.46*\text{Depth of cut} + 3.76*\text{ Depth of cut}^2$

In the ANOVA investigation, the desired level of confidence was considered to be 95%. The model F value of 11.94 implies that the model is significant. There is only a 0.01% chance that a model F value this large could occur due to noise. The "Lack of Fit F-value" of 4.61 implies there is a 5.26% chance that a "Lack of Fit F- value" this large could occur due to noise.

Table 4.4: Analysis of variance for Resultant force after pooling for B_4C composite.

Source	Sum of Squares	DF	Mean Square	F Value	p-value Prob > F	
Model	1046.47	4	261.62	11.94	0.0001	significant
A-Feed rate	*37.21*	*1*	*37.21*	*1.70*	*0.2121*	
B-Speed	*42.21*	*1*	*42.21*	*1.93*	*0.1854*	
C-Depth of cut	*759.37*	*1*	*759.37*	*34.67*	*< 0.0001*	
C^2	*207.69*	*1*	*207.69*	*9.48*	*0.0076*	
Residual	328.56	15	21.90			
Lack of Fit	*296.44*	*10*	*29.64*	*4.61*	*0.0526*	*not significant*
Pure Error	*32.12*	*5*	*6.42*			
Cor Total	1375.03	19				

Std. Dev.	4.68	R-Squared	0.7611
Mean	19.53	Adj R-Squared	0.6973
C.V. %	23.96	Pred R-Squared	0.4712
PRESS	727.15	Adeq Precision	12.942

The goodness of fit of the model was checked by the determination coefficient (R2). The coefficient of determination (R2) was calculated to be 0.7611 for response. This implies that 76.11% of experimental data confirms the compatibility with the data predicted by the model, and the model does not explain only 23.89% of the total variations. The R2 value is always between 0 and 1, and its value indicates correctness of the model. For a good statistical model, R2 value should be close to 1.0. **[32]**

"Adeq Precision" measures the signal to noise ratio. A ratio greater than 4 is desirable. The ratio of 12.942 indicates an adequate signal. This model can be used to navigate the design space.

Fig. 4.20 shows the correlation between the predicted and experimental values for resultant force (R). The normal probabilities of residuals are shown in Fig. 4.21. After the regression model of resultant force was developed, the model adequacy checking was performed in order to verify that the underlying assumption of regression analysis is not violated.

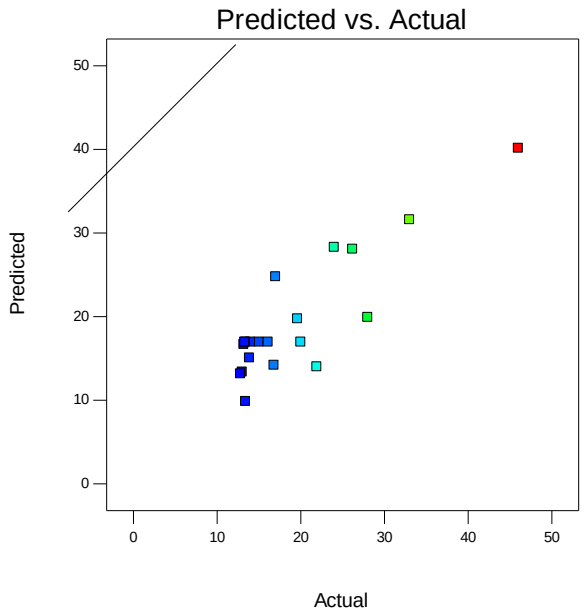

Figure 4.20: Correlation between the predicted and experimental values for B_4C.

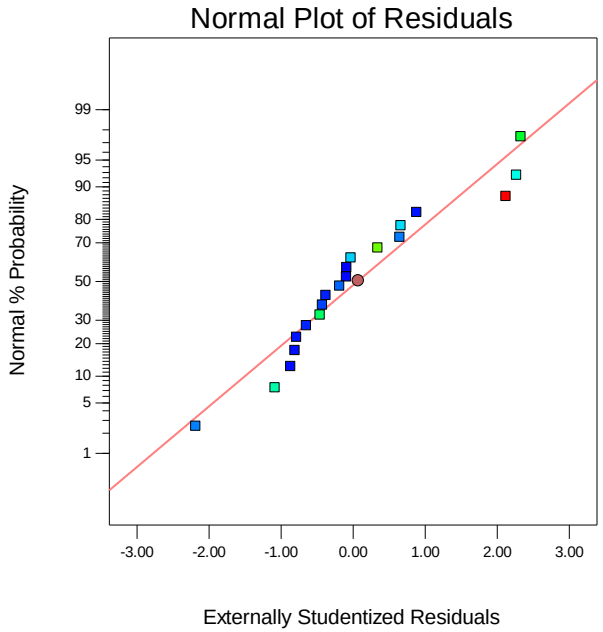

Figure 4.21: The normal probability of residuals for B_4C composite.

Fig. 4.21 illustrates the normal probability plot of the residual, which shows no sign of the violation since each point in the plot follows a straight line pattern. The normal probability plot is used to verify the normality assumption. The data are spread roughly along the straight line. Hence, it is concluded that the data are normally distributed. **[32]**

4.5.1.1 Effect of process parameters on resultant force for B_4C composite

Here the influence of process parameters i.e. speed, feed and depth of cut has been evaluated against resultant force calculated by turning of developed AMC.

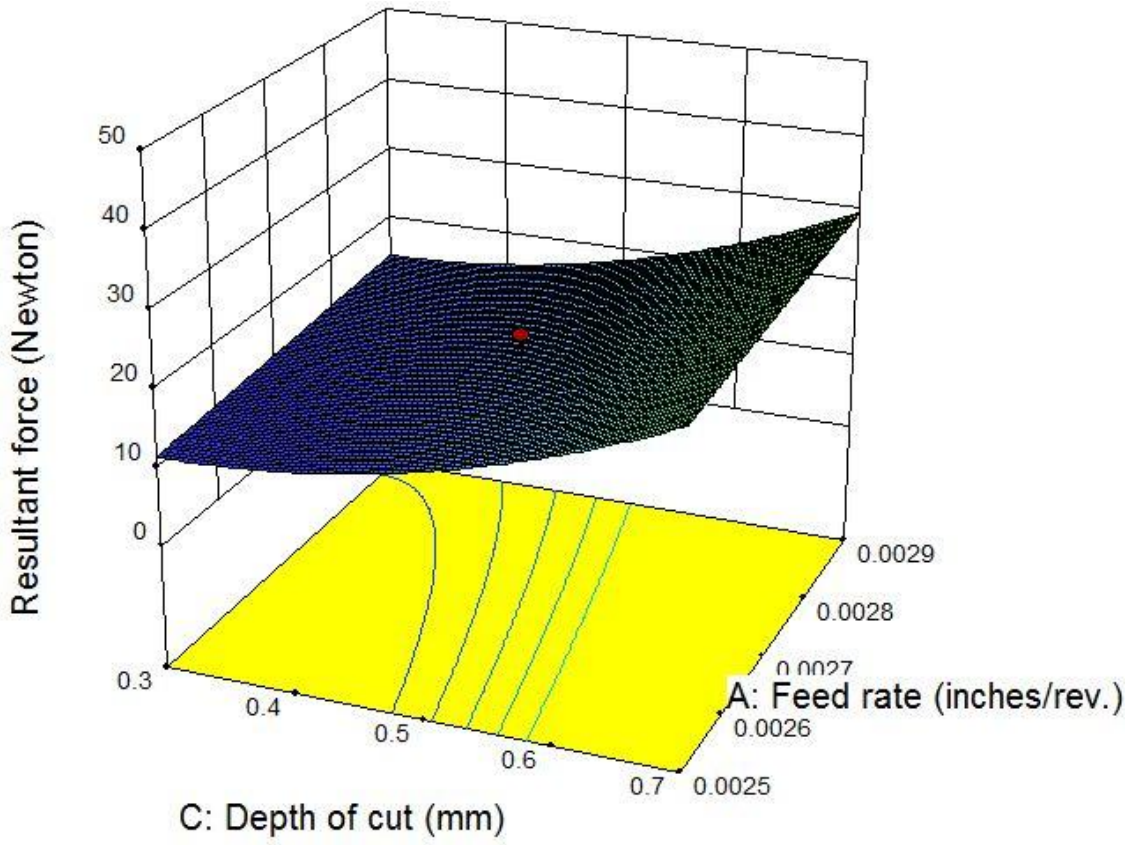

(a)

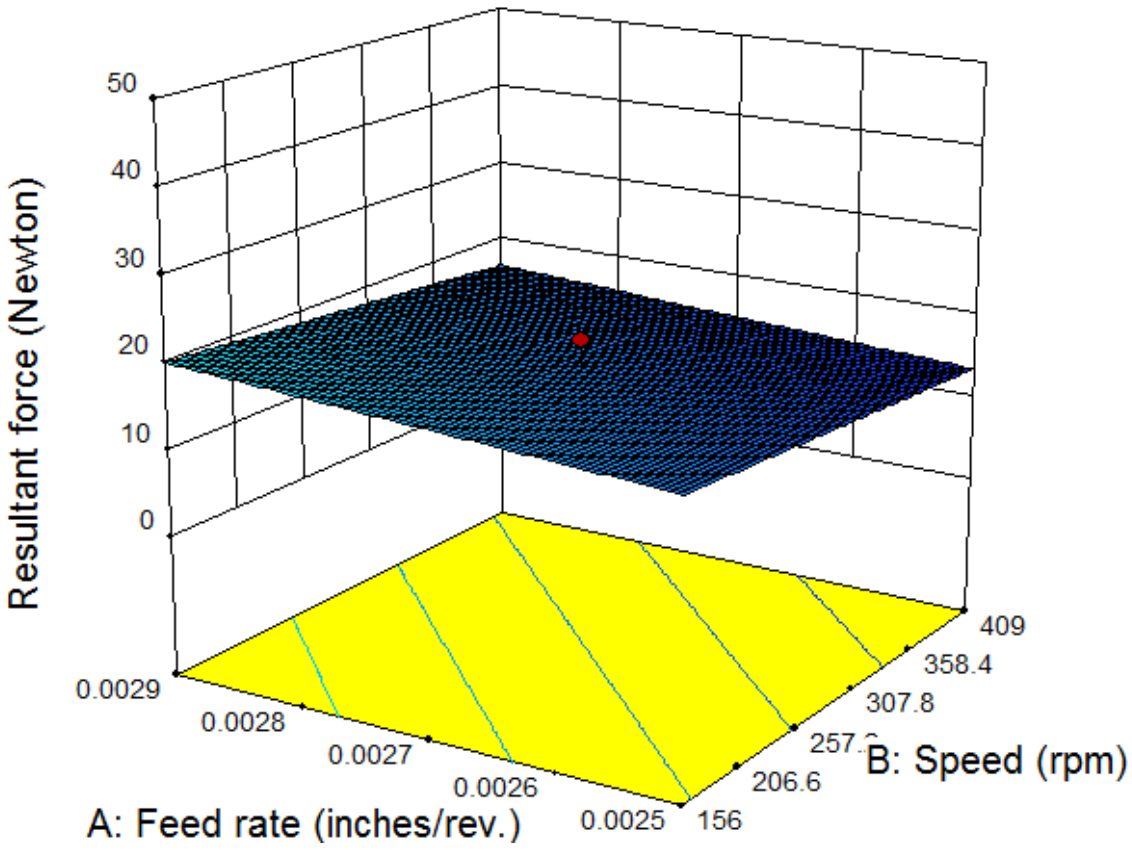

(b)

Figure 4.22: (a) Effect of depth of cut and feed rate on resultant force (b) Effect of feed rate and speed on resultant force for B_4C composite.

It can be seen from figure 4.19 that resultant force increases with increase in depth of cut parabolicaly because of more digging of tool into the work piece and higher chip thickness. Also the resultant force increased with increase in feed rate linearly which is due to increase in MRR. As MRR increase friction developed between tool and material increases and thus higher forces are required for cutting of material. But resultant force decreases linearly with increase in speed because at high speed piercing the metal becomes easier and thus easy material removing. However the decrease is very small.

4.5.2 Analysis of machining for AA7075

After the analysis of machining for B_4C composite, the analysis was done for as casted AA7075. Design matrix and values of resultant force for AA7075 is in table 4.5

Table 4.5: Design matrix and Experimental results for AA7075

		Factor 1	Factor 2	Factor 3	Response 1
Std	Run	A:Feed rate	B:Speed	C:Depth of cut	R1
		inches/rev	rpm		
1	1	0.0025	156	0.3	12
2	2	0.0029	156	0.3	12.5
3	6	0.0025	409	0.3	12.4
4	9	0.0029	409	0.3	12.7
5	11	0.0025	156	0.7	22
6	19	0.0029	156	0.7	22
7	13	0.0025	409	0.7	14
8	14	0.0029	409	0.7	21
9	17	0.0023	282	0.5	13
10	3	0.0030	282	0.5	15
11	15	0.0027	69	0.5	25
12	7	0.0027	495	0.5	14.3
13	8	0.0027	282	0.16	13.87
14	20	0.0027	282	0.83	40.4
15	16	0.0027	282	0.5	14.3
16	5	0.0027	282	0.5	14.2
17	4	0.0027	282	0.5	12.9
18	10	0.0027	282	0.5	13.1
19	12	0.0027	282	0.5	17

20	18	0.0027	282	0.5	19

Values of "Prob > F" less than 0.0500 indicate model terms are significant. From table feed, speed, depth of cut and square term of depth of cut are significant model terms. Values greater than 0.1000 indicate the model terms are not significant. The final empirical relationship was constructed using only these coefficients, and the developed final empirical relationship is given below:

$R = +16.96 + 1.65*\text{Feed rate} - 1.76*\text{Speed} + 7.46*\text{Depth of cut} + 3.76*\text{Depth of cut}^2$

In the ANOVA investigation, the desired level of confidence was considered to be 95%. The model F value of 10.17 implies that the model is significant. There is only a 0.01% chance that a model F value this large could occur due to noise. The "Lack of Fit F-value" of 3.48 implies there is a 9.07% chance that a "Lack of Fit F- value" this large could occur due to noise.

Table 4.4: Analysis of variance for Resultant force after pooling for AA7075

Source	**Sum of Squares**	**DF**	**Mean Square**	**F Value**	**p-value, Prob > F**	
Model	628.11	4	157.03	10.17	0.0003	Significant
A-Feed rate	*9.13*	*1*	*9.13*	*0.59*	*0.4539*	
B-Speed	*51.02*	*1*	*51.02*	*3.30*	*0.0891*	
C-Depth of cut	*401.17*	*1*	*401.17*	*25.99*	*0.0001*	

C^2	*166.80*	*1*	*166.80*	*10.80*	*0.0050*	
Residual	231.57	15	15.44			
Lack of Fit	*202.46*	*10*	*20.25*	*3.48*	*0.0907*	*not significant*
Pure Error	*29.11*	*5*	*5.82*			
Cor Total	859.67	19				

Std. Dev.	3.93	R-Squared	0.7306
Mean	17.03	Adj R-Squared	0.6588
C.V. %	23.07	Pred R-Squared	0.2977
PRESS	603.76	Adeq Precision	11.936

The goodness of fit of the model was checked by the determination coefficient (R2). The coefficient of determination (R2) was calculated to be 0.7306 for response. This implies that 73.06% of experimental data confirms the compatibility with the data predicted by the model, and the model does not explain only 26.94% of the total variations.

"Adeq Precision" measures the signal to noise ratio. A ratio greater than 4 is desirable. The ratio of 12.942 indicates an adequate signal. This model can be used to navigate the design space.

Fig. 4.23 shows the correlation between the predicted and experimental values for resultant force (R). The normal probabilities of residuals are shown in Fig. 4.24

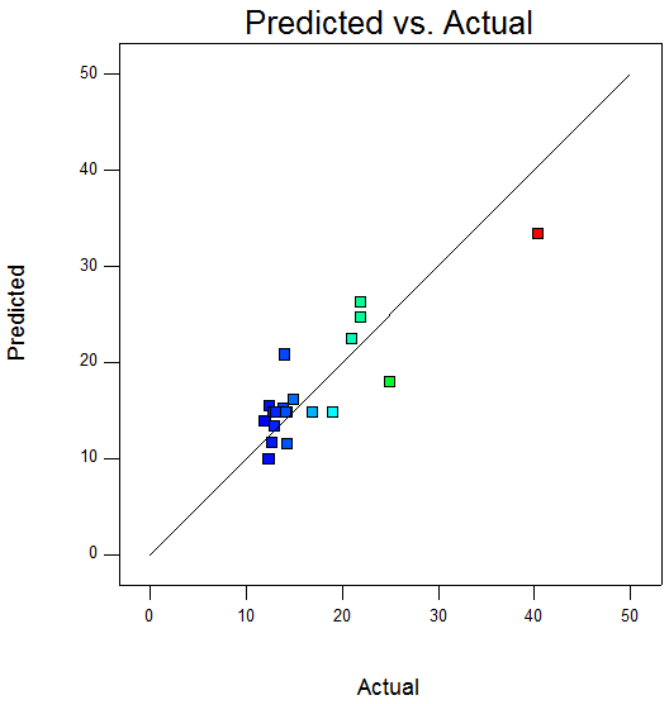

Figure 4.23: Correlation between the predicted and experimental values for AA7075.

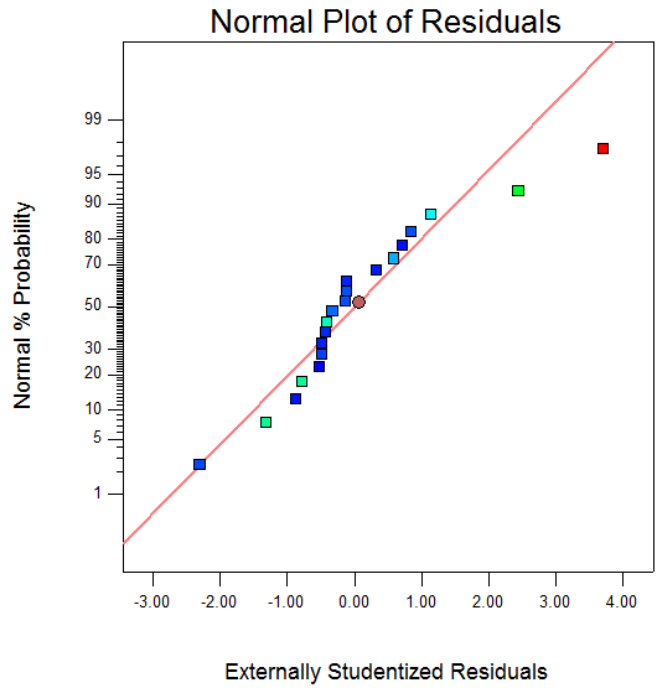

Figure 4.24: The normal probability of residuals for AA7075.

4.5.2.1 Effect of process parameters on resultant force for AA7075

The effect of process parameters was same in this case as in analysis of B_4C composite. The variation and influence of speed, feed and depth of cut has been shown in figure 4.25

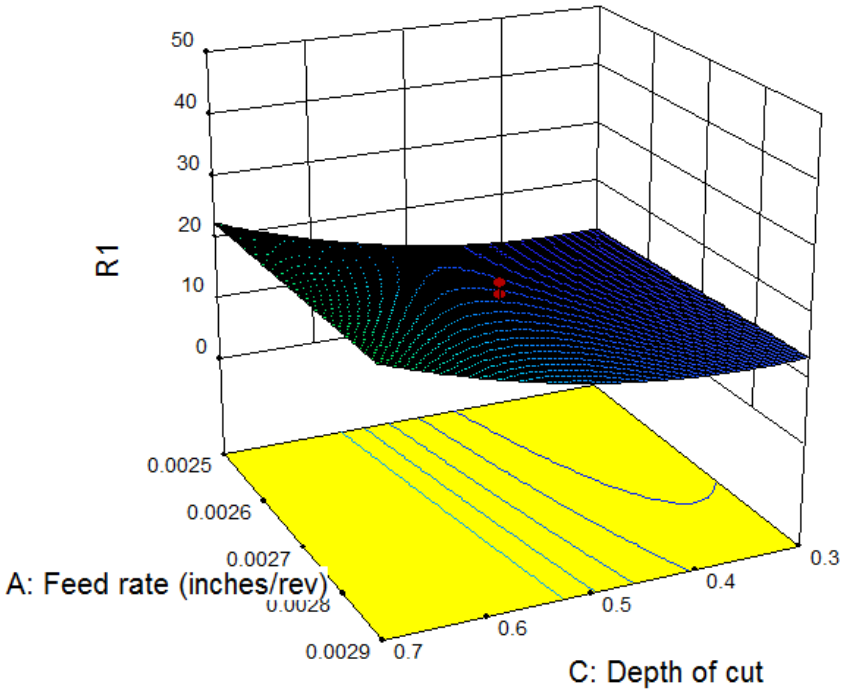

(a)

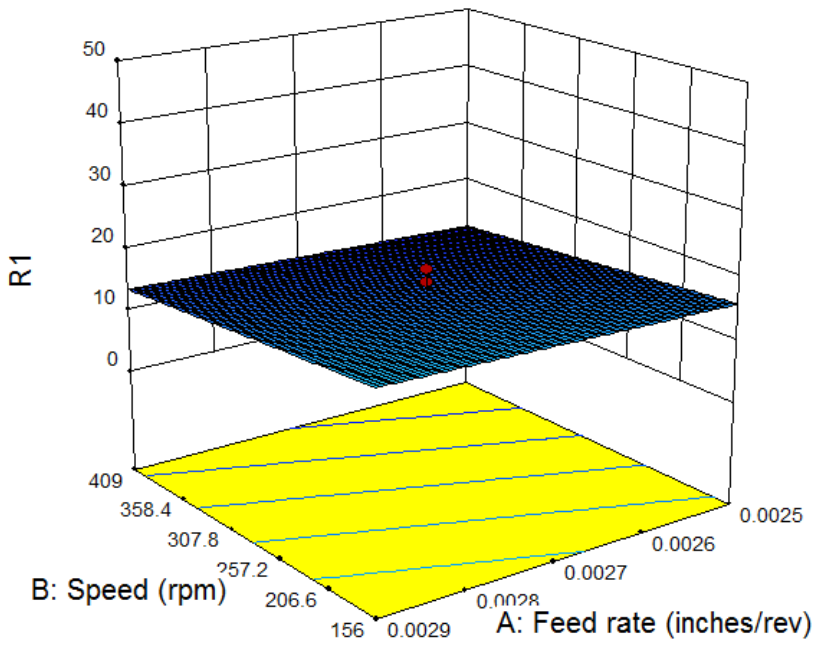

(b)

Figure 4.25: (a) Effect of depth of cut and feed rate on resultant force (b) Effect of feed rate and speed on resultant force for AA7075.

4.5.3 Confirmation Experiments

By analyzing the resulatant force values in both cases the maximium value of resultant force was found at following values of the cutting parameters: speed of 282 rpm, feed of 0.0027 inches/rev. and depth of cut 0.83 mm for both cases. Three confirmation experiments were conducted at the optimum setting of cutting parameters. The average value of resultant force was found to be be 49 N and 44 N for B_4C composite and as-casted AA7075 respectively.

Also the resultant force values for B_4C composite and as-casted AA7075 respectively show that machining becomes difficult in case of B_4C composite as higher the force more it is difficult to machine the material. This effect is due to presence of B_4C particles on the surface of composite developed. As the hard B_4C particles provide resistance to removal of material from the composite surface.

CHAPTER-6

CONCLUSIONS

After doing the whole experimental part and investigation of different properties, the following conclusions have been made:

1. Defect free aluminium metal matrix composite was fabricated by Stir casting method with AA7075 as matrix phase and B_4C as dispersed phase.
2. Microstructure studies show uniform distribution of B_4C particles into the matrix. Also the grain the size reduction was observed with the addition of reinforcement particles.
3. The Vicker's hardness value of the composite increased with inclusion of hard phase B_4C particles. An increase of 9% with addition of 5% of B_4C particles was reported as compared to as-casted AA7075.
4. Furthermore, the tensile strength and yield strength increased with the introduction of particles. An increase of 40% and 29% was reported for tensile strength and yield strength respectively.
5. The ductility (percentage elongation) of the composite decreased with the addition of hard phase reinforcement particles. The percentage elongation decreased from 2.67 % for as-casted sample to 1.40 % for the B_4C composite.
6. Incorporation of B4C particles in the aluminium matrix as a reinforcement decreases the wear rates of the composite compared to as cast 7075 alloy. Coefficient of friction is stabilized with incorporation of B4C in Al 7075 alloy.
7. Wear rate decreases as the sliding speed increases up to transition speed and load, due to work hardening of the surface, formation of Iron oxide and crushing of the B4C particles and smearing of Graphite. Seizure occurred for wrought aluminium based alloys, but no seizure occurred for Al/ B4Cp powder composites under the present study.

8. An empirical relationship was developed to predict the resultant force incorporating machining parameters at 95% confidence level for both AMC and as-casted AA7075. It was observed that the parameters which affect the resultant force in descending order are: depth of cut, feed and speed in both cases.
9. The ANOVA also revealed that feed, speed, depth of cut and square of depth of cut has a significant effect.
10. The best combination of experiments for resultant force (at 46 N for B_4C composite and 40.4 N for AA7075) was found to be speed of 282 rpm, feed of 0.0027 inches/rev. and depth of cut 0.83 mm. The confirmation experiment done on these values show resultant force to be 49 N and 44 N for B_4C composite and as-casted AA7075 respectively.
11. Also the resultant force values for B_4C composite and as-casted AA7075 respectively show that machining becomes difficult in case of B_4C composite.

REFERENCES

1. N. Valibeygloo, R. Azari Khosroshahi, and R. Taherzadeh Mousavian, "Microstructural and mechanical properties of Al-4.5wt% Cu reinforced with alumina nanoparticles by stir casting method," Int. J. Miner. Metall. Mater., vol. 20, no. 10, pp. 978–985, 2013.

2. J. Hashim, L. Looney, and M. S. J. Hashmi, "Metal matrix composites: production by the stir casting method," J. Mater. Process. Technol., vol. 92–93, pp. 1–7, 1999.

3. S. Naher, D. Brabazon,L. Looney "SIMULATION OF THE STIR CASTING PROCESS," CJournal Mater. Process. Technol., no. 5, pp. 567–571, 2003.

4. K. Sekar, Allesu K., and M.A. Joseph, "Design of a stir casting machine," Am. Int. J. Res. Sci. Technol. Eng. Math., vol. 13, no. 214, pp. 56–62, 2013.

5. A. T. Thomas, R. Parameshwaran, A. Muthukrishnan, and M. A. Kumaran, "Development of Feeding & Stirring Mechanisms for Stir Casting of Aluminium Matrix Composites," Procedia Mater. Sci., vol. 5, pp. 1182–1191, 2014.

6. S. H. Juang, L.-J. Fan, and H. P. O. Yang, "Influence of preheating temperatures and adding rates on distributions of fly ash in aluminum matrix composites prepared by stir casting," Int. J. Precis. Eng. Manuf., vol. 16, no. 7, pp. 1321–1327, 2015.

7. O. Beffort, S. Long, C. Cayron, J. Kuebler, and P. A. Buffat, "Alloying effects on microstructure and mechanical properties of high volume fraction SiC-particle reinforced Al-MMCs made by squeeze casting infiltration," Compos. Sci. Technol., vol. 67, no. 3–4, pp. 737–745, 2007.

8. N. Barman and P. Dutta, "Evolution of microstructure during solidification of an aluminium alloy under stirring," Trans. Indian Inst. Met., vol. 65, no. 6, pp. 683–687, 2012.

9. H. R. Ezatpour, S. A. Sajjadi, M. H. Sabzevar, and Y. Huang, "Investigation of microstructure and mechanical properties of Al6061-nanocomposite fabricated by stir casting," Mater. Des., vol. 55, pp. 921–928, 2014.

10. S. B. Hassan and V. S. Aigbodion, "Effects of eggshell on the microstructures and properties of Al–Cu–Mg/eggshell particulate composites," J. King Saud Univ. - Eng. Sci., vol. 27, no. 1, pp. 49–56, 2015.

11. N. Valibeygloo, R. Azari Khosroshahi, and R. Taherzadeh Mousavian, "Microstructural and mechanical properties of Al-4.5wt% Cu reinforced with alumina nanoparticles by stir casting method," Int. J. Miner. Metall. Mater., vol. 20, no. 10, pp. 978–985, 2013.

12. S. Suresh and N. S. V. Moorthi, "Process development in stir casting and investigation on microstructures and wear behavior of TiB2 on A16061 MMC," Procedia Eng., vol. 64, pp. 1183–1190, 2013.

13. R. Flores-Campos, I. Estrada-Guel, M. Miki-Yoshida, R. Martínez-Sánchez, and J. M. Herrera-Ramírez, "Microstructure and mechanical properties of 7075 aluminum alloy nanostructured composites processed by mechanical milling and indirect hot extrusion," Mater. Charact., vol. 63, pp. 39–46, 2012.

14. S. D. Saravanan and M. S. Kumar, "Effect of Mechanical Properties on Rice Husk Ash Reinforced Aluminum Alloy (AlSi10Mg) Matrix Composites," Procedia Eng., vol. 64, pp. 1505–1513, 2013.

15. A. Kumar, S. Lal, and S. Kumar, "Original article Fabrication and characterization of A359 / Al 2 O 3 metal matrix composite using electromagnetic stir casting method," Integr. Med. Res., vol. 2, no. x x, pp. 3–7, 2013.

16. M. Karbalaei Akbari, H. R. Baharvandi, and K. Shirvanimoghaddam, "Tensile and fracture behavior of nano/micro TiB2 particle reinforced casting A356 aluminum alloy composites," Mater. Des., vol. 66, pp. 150–161, 2015.

17. I. Balasubramanian and R. Maheswaran, "Effect of inclusion of SiC particulates on the mechanical resistance behaviour of stir-cast AA6063/SiC composites," Mater. Des., vol. 65, pp. 511–520, 2015.

18. V. Balaji, N. Sateesh, and M. M. Hussain, "Manufacture of Aluminium Metal Matrix Composite (Al7075-SiC) by Stir Casting Technique," Mater. Today Proc., vol. 2, no. 4–5, pp. 3403–3408, 2015.

19. A. Viswanath, H. Dieringa, K. K. Ajith Kumar, U. T. S. Pillai, and B. C. Pai, "Investigation on mechanical properties and creep behavior of stir cast AZ91-SiCp composites," J. Magnes. Alloy., vol. 3, no. 1, pp. 16–22, 2015.

20. B. Ravi, B. B. Balu Naik, and J. Udaya Prakash, "Characterization of Aluminium Matrix Composites (AA6061/B4C) Fabricated by Stir Casting Technique," Mater. Today Proc., vol. 2, no. 4–5, pp. 2984–2990, 2015.

21. S. Aravindan, P. V Rao, and K. Ponappa, "Evaluation of physical and mechanical properties of AZ91D/SiC composites by two step stir casting process," J. Magnes. Alloy., vol. 3, no. 1, pp. 52–62, 2015.

22. K. Mahadevan, K. Raghukandan, T. Senthilvelan, B. C. Pai, and U. T. S. Pillai, "Investigations on the high cycle fatigue behaviour of stir cast AA 6061-SiCp composites," J. Mater. Sci., vol. 41, no. 17, pp. 5548–5555, 2006.

23. S. Gopalakrishnan and N. Murugan, "Production and wear characterisation of AA 6061 matrix titanium carbide particulate reinforced composite by enhanced stir casting method," Compos. Part B Eng., vol. 43, no. 2, pp. 302–308, 2012.

24. S. Kumar, R. S. Panwar, and O. P. Pandey, "Effect of dual reinforced ceramic particles on high temperature tribological properties of aluminum composites," Ceram. Int., vol. 39, no. 6, pp. 6333–6342, 2013.

25. V. Sivananth, S. Vijayarangan, and N. Rajamanickam, "Evaluation of fatigue and impact behavior of titanium carbide reinforced metal matrix composites," Mater. Sci. Eng. *A*, vol. 597, pp. 304–313, 2014.

26. M. F. Ibrahim, H. R. Ammar, a. M. Samuel, M. S. Soliman, and F. H. Samuel, "On the impact toughness of Al-15 vol.% B4C metal matrix composites," Compos. Part B Eng., vol. 79, pp. 83–94, 2015.

27. A. Manna and B. Bhattacharayya, "Influence of machining parameters on the machinability of particulate reinforced Al/SiC-MMC," Int. J. Adv. Manuf. Technol., vol. 25, no. 9–10, pp. 850–856, 2005.

28. E. Kiliçkap, O. Çakir, M. Aksoy, and A. Inan, "Study of tool wear and surface roughness in machining of homogenised SiC-p reinforced aluminium metal matrix composite," J. Mater. Process. Technol., vol. 164–165, pp. 862–867, 2005.

29. T. Ozben, E. Kilickap, and O. Çakir, "Investigation of mechanical and machinability properties of SiC particle reinforced Al-MMC," J. Mater. Process. Technol., vol. 198, no. 1–3, pp. 220–225, 2008.

30. S. Kannan, H. A. Kishawy, and I. Deiab, "Cutting forces and TEM analysis of the generated surface during machining metal matrix composites," J. Mater. Process. Technol., vol. 209, no. 5, pp. 2260–2269, 2009.

31. N. Altınkok, "Investigation of mechanical and machinability properties of Al2O3/SiCp reinforced Al-based composite fabricated by stir cast technique," J. Porous Mater., vol. 22, no. 6, pp. 1643–1654, 2015.

32. S. P. Dwivedi, S. Kumar, and A. Kumar, "Effect of turning parameters on surface roughness of A356/5% SiC composite produced by electromagnetic stir casting," J. Mech. Sci. Technol., vol. 26, no. 12, pp. 3973–3979, 2012.